Deformation Strengthening of Uranium and Dilute Uranium Alloys

Eckelmeyer, Kenneth H.
Dudder, Gordon B.
Chapman, Lloyd R.
Ludtka, Gerard M.
O'Brien, Mary Kathleen

To be published in: Journal of Nuclear Materials

DOI to publisher's version: 10.1016/j.jnucmat.2023.154825

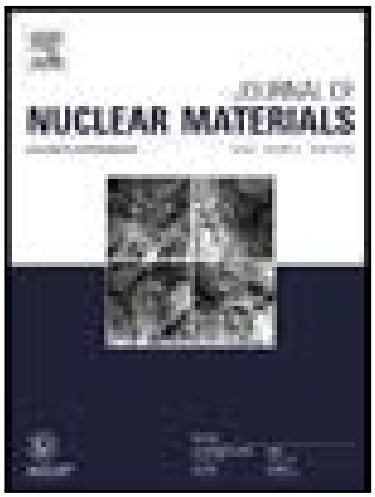

Deformation Strengthening of Uranium and Dilute Uranium Alloys

Kenneth H. Eckelmeyer , Gordon B. Dudder , Lloyd R. Chapman , Gerard M. Ludtka , Mary K. O'Brien

PII: S0022-3115(23)00592-5
DOI: https://doi.org/10.1016/j.jnucmat.2023.154825
Reference: NUMA 154825

To appear in: *Journal of Nuclear Materials*

Received date: 29 August 2023
Revised date: 17 November 2023
Accepted date: 19 November 2023

Please cite this article as: Kenneth H. Eckelmeyer , Gordon B. Dudder , Lloyd R. Chapman , Gerard M. Ludtka , Mary K. O'Brien , Deformation Strengthening of Uranium and Dilute Uranium Alloys, *Journal of Nuclear Materials* (2023), doi: https://doi.org/10.1016/j.jnucmat.2023.154825

Deformation Strengthening of Uranium and Dilute Uranium Alloys

Kenneth H. Eckelmeyer (a)
Gordon B. Dudder (b)
Lloyd R. Chapman (c)
Gerard M. Ludtka (c)
Mary K. O'Brien (d)

11/15/2023

a) Formerly Sandia National Laboratory, Albuquerque, NM, USA
b) Formerly Pacific Northwest National Laboratory, Richland, WA, USA
c) Formerly U.S. Department of Energy, Y-12 Plant, Oak Ridge, TN, USA
d) Los Alamos National Laboratory, Los Alamos, NM, USA

Abstract

The strength and ductility of uranium and dilute uranium alloys can be substantially improved by deformation strengthening. The yield strength of unalloyed uranium can be nearly doubled by rolling in the vicinity of 250°C. The embrittling effect of hydrogen is also overcome, eliminating the need for vacuum outgassing to obtain good ductility. Significant differences in longitudinal versus transverse tensile properties result, in part, from texture introduced by unidirectional rolling. Warm rolling of U-2.3%Nb results in both traditional strain hardening and a significant Bauschinger effect, resulting in differences between tensile and compressive yield strength. A similar combination of strain hardening and Bauschinger effect also occurs in deformation strengthened U-0.75%Ti. Warm rolling of U-0.75%Ti results in significantly better combinations of tensile yield strength and ductility than can be obtained by conventional age hardening. Warm rolling prior to aging also reduces the loss of ductility which typically accompanies conventional age hardening. An approach is developed in which the effects of prior deformation on tensile and compressive yield strengths are analyzed in terms of texture, long-range dislocation, and Bauschinger effects. The Bauschinger effect is shown to vary in sign with the type of deformation, thus providing opportunities to tailor tensile and compressive properties.

1. Introduction

Uranium and dilute uranium alloys are used for a variety of applications based on their high densities (>18 g/cm^3) and their special nuclear properties (Ref. 1). U-0.75%Ti is commonly used for applications requiring intermediate to high yield strengths (700 to 1000 MPa). This alloy is typically γ-solution heat treated at 800°C, quenched to obtain a supersaturated martensitic variant of α-phase, then age hardened in the vicinity of 380°C.

The alternative approach of deformation strengthening has received relatively little attention. Unalloyed uranium can be rolled or swaged at room temperature, but the single (010) [100] slip system operative below ~200°C limits the amount of deformation that can be practically achieved. Much higher reductions are possible at temperatures between ~250°C, where additional slip systems come into play, and ~525°C, where dynamic recrystallization occurs. Early work showed that rolling in the 250°C to 300°C range decreased the ductile-to-brittle transition temperature, thus improving tensile ductility in the vicinity of room temperature (Refs. 2-3). This phenomenon was later investigated in greater detail, where tensile properties were assessed for material that had been rolled up to 90% reduction at 250°C (Ref. 4). Strength and ductility were both found to increase with increased amounts of warm working. The tensile elongations corresponding to various amounts of warm working varied somewhat, likely due to differences in test sample geometry. But elongations of at least ~20% were consistently obtained in material that had been reduced 60% or more at 250°C. The authors attributed this high ductility to dislocation substructure, speculating that the resulting 0.36 to 0.46 micrometer cells observed by transmission electron microscopy served to reduce “effective grain size”, thus increasing both strength and ductility (Refs. 4-5).

Very little work on deformation strengthening of uranium alloys has been reported in the open literature. Compressive upsetting has been used primarily as a mechanical stress leveling approach for reducing quenching-induced residual stresses (Ref. 6). Axial tensile tests (antiparallel to the prior compressive strain) on U-2.3%Nb cylinders that had been upset ~3% after slow cooling showed only slight changes in yield and ultimate strength (Ref. 7). Axial tensile and compression tests on U-0.75%Ti cylinders that had been upset 1% to 3% after γ-quenching showed very limited changes in tensile properties, but up to ~300 MPa increases in compressive yield strength (Ref. 8). These large difference between tensile and compressive behavior suggested that a Bauschinger effect may significantly influence the properties of deformation strengthened material.

The results presented here represent a synthesis of several previously unpublished projects designed to investigate the potential of deformation strengthening of unalloyed uranium, U-2.3% Nb, and U-0.75%Ti. A potential advantage of deformation strengthening in unalloyed uranium and U-2.3%Nb was avoiding the quenching step required for conventional heat treatment of U-0.75%Ti and the associated limitations in section thickness. Deformation strengthening of previously quenched U-0.75%Ti provided potential for improved mechanical properties of α'_b martensite, perhaps augmented by aging.

The effects of deformation temperature and deformation amount were assessed for all three materials. The possibility of deformation strengthening combined with age hardening was also investigated for U-0.75%Ti. An approach was also developed to separate and assess the various components that contribute to strengthening in uranium alloys.

2. Experimental

Large (>500 kilogram) ingots of unalloyed uranium, U-2.3%Nb, and U-0.75%Ti were produced by vacuum induction melting. Uranium derbies and high purity alloying elements were melted in zirconia washed graphite crucibles and bottom poured into zirconia washed graphite molds, as described elsewhere (Ref. 9). The resulting ingots were converted to plate by a series of hot forging, rolling, and recrystallization steps to break down the cast microstructure and provide wrought material for subsequent deformation strengthening experiments. Chemical compositions of the U-2.3%Nb and U-0.75Ti alloys are shown in Table 1. No chemical analyses were available for the unalloyed uranium, but a typical specification for material produced by this method is also included in Table 1.

2.1. Unalloyed Uranium

The unalloyed uranium castings were heated in molten salt, unidirectionally hot rolled using 25.4 cm diameter rolls starting at 630°C (in the high α-range), and repeatedly annealed, resulting in a starting microstructure consisting of ~10 um equiaxed grains. These plates were reheated to 630°C in molten salt in preparation for the final deformation strengthening sequence. A limited number of samples were also annealed in vacuum at 630°C for 2 hours or 300°C for 24 hours to remove at least 90% of the hydrogen. Comparison of the vacuum annealed samples with those from material heated in salt provided a basis for assessing how 1 to 2 weight ppm hydrogen, which is predictably picked up from small amounts of moisture in the salt bath (Refs. 10-13), influenced the ductility of the starting material.

Plates that had been preheated to 630°C in molten salt were unidirectionally rolled in ~10% passes using 25.4 cm rolls to total reductions ranging from 60% to 93.5% -- the warm rolling direction was consistently the same as the rolling direction during prior ingot breakdown. Infrared temperature measurements were made on entry and exit from the mill during each pass. Some cooling occurred during transfer from the salt bath to the rolling mill, resulting in an initial pass temperature of ~550°C. Slight heating occurred during each pass, and additional cooling occurred between passes. During a typical baseline rolling sequence to 60% total reduction the final pass occurred at 350°C. Lower finishing temperatures were achieved by increasing the transfer time prior to the first pass, as well as the delay times between passes. Reductions greater than 60% were obtained using thicker starting plates so that samples representing different total reductions finished at similar thicknesses, permitting tensile samples of uniform thickness to be tested. The material temperature after the final pass was recorded and used as

characteristic of the rolling process, consistent with the assumption that the last passes were the most consequential in terms of property development. Metallographic examination of cross sectioned rolled plates revealed severely flattened and elongated grains, confirming that dynamic recrystallization had not occurred. Flat tensile samples were machined parallel and transverse to the rolling direction.

2.2. U-2.3%Nb

The starting material for the study of U-2.3%Nb were plates that had been broken down by hot upset forging at 900°C followed by hot rolling at 800°C (both in the γ-range). The plates were then vacuum annealed at 800°C to reduce hydrogen content and furnace cooled to room temperature. Pseudo-equilibrium monotectoid decomposition of the γ-phase occurred during slow cooling, resulting in a starting microstructure consisting primarily of a two-phase semi-lamellar mixture of essentially pure α-uranium and an alloy-enriched γ-phase, as shown in Figure 1. The annealed plates were heated in dry argon to temperatures up to 500°C, and unidirectionally rolled in ~5% to ~10% passes using 25.4 cm diameter rolls to total reductions ranging from 5% to 70.5% (~5% passes were employed during rolling at 25°C and 155°C, ~10% passes at higher rolling temperatures). Plates were re-equilibrated at temperature for ~10 minutes after each pass, making rolling essentially isothermal. Standard 6.35 mm gage diameter round tensile and compression samples were machined parallel to the rolling direction and tested in the as-rolled condition A limited number of tensile and compressive tests were also done on material that had been reduced 20% at 25°C and 66% at 265°C and subsequently heat treated for one hour at temperatures ranging from 150°C to 550°C.

2.3. U-0.75%Ti

The starting material for the study of U-0.75%Ti were plates that had been broken down by hot upset forging at 900°C (in the γ-range), followed by hot rolling at 630°C (in the high α-range). These were vacuum annealed at 800°C to reduce hydrogen content, then water quenched to room temperature. Martensitic transformation of the γ-phase occurred during quenching, resulting in an acicular martensitic a'_a microstructure, as shown in Figure 2.

A limited number of small samples machined to tapered thickness were rolled using 12.7 cm diameter rolls to uniform final thicknesses, thus producing a continuous range of reductions. These were used to screen the effects of rolling temperature and reduction on hardness, as well as the effects of subsequent aging on hardness.

Larger plates of uniform thickness were heated to temperatures up to 350°C, then unidirectionally rolled in ~5% to 10% passes using 25.4 cm diameter rolls to total reductions ranging from 5% to 50% (~5% passes were employed during rolling at 25°C, ~10% passes at 250°C and above). Plates were returned to the furnace for ~5 minutes after each pass, making rolling essentially isothermal. Some samples were tested as-rolled, while others were given additional aging treatments prior to testing. Standard 6.35 mm gage diameter round tensile and compression samples were machined parallel to the rolling direction for most processes. Transverse tensile samples were also prepared for two processes.

2.4. Mechanical Testing

All mechanical tests were conducted at room temperature in dry air at typical quasi-static rates (~10^{-3}/sec). Each test result represents the average of at least two tests.

3. Results

3.1. Unalloyed Uranium

3.1.1. Effect of Hydrogen on Annealed Ductility

The annealing environment and resulting hydrogen content had a profound effect on the room temperature tensile ductility of annealed uranium, as can be seen by comparing rows 1 and 2 in Tables 2a and 2b. Material that had been heated to 630°C in molten salt exhibited less than 10% elongation and reduction in area. But material that had been vacuum annealed at 630°C exhibited elongations greater than 20% and reductions in area exceeding 35%. These differences were attributable to dissolved hydrogen, which is picked up during heating in molten salt, but removed by vacuum annealing, as has been previously documented (Refs. 10-13).

It is important to note that all of the material used in the deformation strengthening experiments was heated in molten salt in preparation for rolling. As a result, hydrogen concentrations between 1 to 2 weight ppm were characteristic of all the deformation strengthened samples, as shown in the 5th columns of Tables 2a and 2b.

3.1.2. Effect of Warm Working on Tensile Properties

Rolling experiments showed that unalloyed uranium could be readily rolled to reductions as high as 93.5% when the finishing temperature was 250°C or higher. Rolling became increasingly difficult at 200°C and lower. Because of this, 60% was the maximum reduction that could be achieved at finishing temperatures below 250°C. Even 60% reduction caused the mill to be severely strained at finishing temperatures of 150°C and lower. Based on this, it was concluded that ~220°C represents the lowest temperature at which unalloyed uranium can realistically be warm rolled to reductions of 60% or higher using 25.4 cm diameter working rolls.

The tensile properties of warm rolled unalloyed uranium are summarized in Table 2, and the effects of rolling temperature and reduction are plotted in Figures 3 to 6. Throughout this paper the tables refer to rolling reductions in engineering terms (% reduction in thickness), but plots provide properties plotted as functions of true strain, with the corresponding engineering reductions noted in the figure captions. Absolute values of true strain were computed using the relationship, $\varepsilon_t = \ln [1 - (\%\ \text{reduction}/100)]$.

Several things are noteworthy in Table 2 and Figures 3-6.

Warm working overcame the embrittling effect of dissolved hydrogen. All of the warm worked samples (which had been heated in molten salt in preparation for warm rolling) exhibited substantially higher elongations and reductions-in-area than those of the unworked high hydrogen starting material. Elongations of rolled samples finished at 250°C or higher ranged from 18% to 35% and reductions-in-area ranged from 38% to 55%. These are dramatically higher than the 5% to 8% values characteristic of material that had been heated in salt and left unworked (Table 2).

Yield and ultimate strength both increased with increasing amounts of warm working. Ductility decreased somewhat, but not dramatically. Figure 3 shows that yield and ultimate strength increased roughly linearly with increasing rolling at 350°C when deformation amount was plotted as true strain (the most meaningful parameter for the large compressive reductions of 60% to 93.5%). Figure 4 shows that elongation decreased slightly with increasing warm deformation. Reductions-in-area were somewhat more scattered, especially in the longitudinal direction.

Strength increased as finishing temperature decreased below 350°C, but this effect plateaued at ~250°C, as shown in Figure 5. Additional increases occurred at finishing temperatures below ~150°C, but significant rolling reductions at these low temperatures were deemed to be impractical. Ductility decreased with decreasing finishing temperature, as shown in Figure 6. Excellent combinations of workability, strength, and ductility were obtained at finishing temperatures in the 250°C to 300°C range.

Significant differences were observed in longitudinal vs. transverse properties. Figures 3 and 5 show that transverse yield strengths were slightly higher than longitudinal ones (~45 MPa average). But much more significant differences were observed in ultimate strength and elongation. Figures 3 and 5 show that transverse ultimate strengths were dramatically lower than the corresponding longitudinal ultimate strengths (by 205 MPa average). In addition, transverse elongations dramatically exceeded their longitudinal counterparts, as shown in Figures 4 and 6. The combination of slightly higher yield strengths, lower ultimate strengths, and greater elongations indicated that strain hardening was much lower in the transverse direction than in the longitudinal direction. The lower ultimate strengths and higher ductilities observed in the transverse direction may have resulted, in part, because very little increase in width occurred during rolling, i.e., rolling resulted in near-zero transverse strain. But similar directional differences were seen even in vacuum annealed material (compare the 2nd rows of Tables 2a and 2b). This suggests that these directional differences were due, to at least some extent, to preferred crystallographic orientation introduced during the ingot breakdown processes and later accentuated as warm working further intensified preferred orientation. The likely role of preferred orientation on property directionality will be discussed in Section 4.1.2.

3.2. U-2.3%Nb

It was found that U-2.3%Nb in the annealed condition could be rolled to 20% reduction at 25°C, to 50% reduction at 155°C, and to more than 65% reduction at 265°C and higher.

Metallographic examination of longitudinally sectioned rolled plates showed that uniform deformation occurred at all temperatures. An example of material rolled at 265°C is shown in Figure 7,

The effects of rolling temperature and rolling reduction on longitudinal tensile and compressive properties are plotted in Figures 8 to 17 – no transverse samples were machined or tested. Yield and ultimate strengths generally increased with increasing reduction, but the extent of strengthening decreased with increasing rolling temperature. Considerable scatter was observed in both tensile elongation and reduction in area. Elongation generally decreased with increasing reduction, most prominently at the lower rolling temperatures. Reduction in area remained relatively unchanged with reduction at 265°C and lower, and actually increased slightly with reduction at 375°C and 500°C.

Compressive yield strength was slightly lower than tensile yield strength in the annealed starting material, and this difference became progressively greater with increased rolling reduction at 25°C and 155°C, as can be seen in Figures 8 and 10. Similar divergences between compressive and tensile yield strengths occurred after initial rolling at 265°C and 375°C, but were no longer seen after higher reductions, as is apparent in Figures 12 and 14. Rolling at 500°C resulted in compressive yield strengths somewhat higher than their tensile counterparts, as shown in Figure 16. This reversal will be discussed in Section 4.2.

3.3. U-0.75%Ti

It was found that U-0.75%Ti in the as-quenched condition could be rolled to ~15% reduction at 25°C – cracking began to occur at ~20% reduction. The material became much more workable at moderately elevated temperatures – 50% reduction was readily obtainable at 250°C. Rolling was also readily accomplished at 350°C, but time at this temperature had to be limited to 30 minutes to avoid age hardening. No rolling trials were done above 350°C.

Hardness results from tapered thickness samples rolled at 25°C are shown in Figure 18, along with hardnesses achieved by aging at 380°C and 420°C. It can be seen that the increases imparted by rolling and aging were essentially additive up to Rockwell C 48. But as peak aging was approached the effects of deformation began to be annealed out.

Metallographic examination of longitudinally sectioned rolled plates showed that uniform deformation occurred up to ~20% reduction. Increasing amounts of shear strain localization occurred at higher reductions, as illustrated in Figure 19. However, the amounts of strain in these shear bands were relatively modest, indicating that they did not represent adiabatic shear instability, which is known to occur in U-0.75%Ti during compression at strain rates above ~50/sec (Ref. 14) (The strain rate during rolling was in the vicinity of ~1/sec.)

The effects of rolling temperature and true rolling strain on longitudinal tensile properties are plotted in Figures 20 and 21. Yield and ultimate strength increased substantially with increasing reduction at 25°C. Similar but less dramatic increases in strength occurred on rolling at 250°C. Elongation decreased with increasing reduction, but remained greater than 15% even after 50% rolling at 250°C. Reduction-in-area remained nearly constant.in the vicinity of 50%. A limited number of plates rolled at 350°C exhibited properties virtually identical to those rolled at 250°C, provided time at 350°C was limited to one hour to avoid the onset of age hardening.

Table 3 compares transverse and longitudinal tensile properties for lightly and heavily warm worked conditions. Transverse yield and ultimate strengths were slightly lower than their longitudinal counterparts. Transverse ductilities were slightly higher. Both are consistent with transverse strain during rolling being near-zero. Preferred orientation, which was significant in the very heavily worked unalloyed uranium, was apparently not a factor in the U-0.75%Ti plates. Not only had they received much less hot work during ingot breakdown, but they had been γ-solution treated at 800°C and quenched prior to warm rolling – this would be expected to eliminate most vestiges of preferred orientation.

Figures 22 and 23 show the effect of aging on tensile properties of material that had previously been rolled at 250°C – note that the changes occurring at 0% deformation represent conventional age hardening, rather than deformation followed by age hardening. It can be seen that age hardening resulted in increased yield and ultimate strength, but that the magnitude of this effect decreased with increasing prior deformation, and was essentially zero in material that had been heavily rolled prior to aging. Similarly, age hardening resulted in decreased elongation and reduction-in-area, but to a decreasing extent with increasing prior deformation. Aging of material that had been reduced 50% by warm working (0.693 true compressive strain) resulted in virtually no changes in yield strength, ultimate strength, or elongation, and only a modest decrease in reduction-in-area when aged.

Changes in macroscopic fracture morphology and microscopic fracture surface appearance confirmed that the trends in reduction-in-area represented substantial changes in fracture behavior. Table 4 summarizes the effects of processing on fracture behavior, and Figures 24-27 show scanning electron micrographs of typical fracture surfaces.

Failed tensile samples of the undeformed starting material and all deformation strengthened conditions exhibited classic cup and cone fracture surfaces. Shear lips comprised ~75% of the fracture surface in undeformed samples. This decreased slightly with increasing deformation strengthening, but was never less than 60%. In contrast, samples that had been conventionally aged at 400°C exhibited flat fractures with almost no shear lips. Warm working prior to aging resulted in more extensive shear lips, and the extent of shear failure increased with the amount of warm working that preceded aging.

The microscopic appearances of the shear lip and central portions of the fracture surfaces were characterized by scanning electron microscopy.

All shear lips exhibited dimples typical of failure by microvoid coalescence. Shear lip dimples in deformation strengthened samples became slightly finer with increasing deformation amount. The very limited shear lips of conventionally age hardened samples exhibited finer dimples. Even finer dimples were seen on the shear lips of samples that had been heavily warm worked prior to aging.

The central regions of the undeformed starting material and all warm worked samples exhibited 100% dimple rupture, as shown in Figure 24. The only effect of warm working was a slight reduction in dimple size. Conventionally aged samples exhibited nearly 100% quasi-cleavage fracture, as shown in Figure 25. Warm working prior to aging resulted in decreasing amounts of quasi-cleavage and increasing amounts of dimple rupture, as shown in Figures 26 and 27. However, the dimples on these fracture surfaces were typically finer than those in the warm worked samples that had not been subsequently aged.

4. Discussion

4.1. Unalloyed Uranium

The observation that uranium can be readily warm rolled at 250°C or higher, but is difficult to cold roll at room temperature is consistent with the operation of multiple slip systems above ~200°C, but only the single (010)[100] slip system at lower temperatures (Ref. 15).

Figures 3 and 5 show that substantial increases in yield and ultimate tensile strength can be obtained by warm rolling. Figures 4 and 6 show that only modest decreases in ductility accompany these increases in strength. An excellent combination of workability, strength, and ductility occurs at finishing temperatures between 250° and 300°C, where a ~250 MPa increase in yield strength and at least a 180 MPa increase in ultimate strength were obtained while retaining good ductility – at least 18% elongation and 40% reduction in area.

4.1.1. Overcoming Hydrogen Embrittlement

It is noteworthy that high ductility was obtained in all the warm worked unalloyed uranium despite the fact that it had been heated to 630°C in molten salt prior to rolling. Moisture in the molten salt predictably introduces 1 to 2 weight ppm hydrogen and results in significant embrittlement of annealed uranium (Refs. 10, 13). Previous studies have reported that tensile reductions-in-area for alpha-annealed samples tested at typical quasi-static rates gradually decrease from ~45% in hydrogen free samples to ~13% in samples containing 0.25 weight ppm hydrogen, then plateau at ~13% at higher hydrogen contents (Refs. 12, 13). Table 2 shows the even more deleterious effect of hydrogen on the starting material used in this study. But Table 2 and Figure 4 show that ductility after warm working was much higher than that of the starting material, regardless of relatively high hydrogen content.

This is consistent with the results of an earlier study (Ref. 4). However, in this previous study the high ductility of the warm worked material was attributed to dislocation substructure. Those authors speculated that sub-micrometer cells served to reduce "effective grain size", and that the increases in strength and ductility were a result of this very fine "effective grain size" (Refs. 4, 5). However, the fact that the elongations plotted in Figure 4 extrapolate back to the value for unworked material with low hydrogen, while unworked material with higher hydrogen was dramatically less ductile, strongly suggests that the controlling factor is warm working having overcome the embrittling effects of hydrogen, rather than a grain size effect.

Another suggestion was that the elongated grains in the warm worked material reduced the extent to which grain boundaries were subject to tensile stress, thereby making the material more resistant to hydrogen embrittlement (Ref 16). This might have merit regarding longitudinal ductility. But the observation that transverse ductility of warm worked material was even higher than longitudinal ductility (compare rows 3, 5, and 6 of Table 2b with the corresponding rows in Table 2a) is not consistent with this.

A more likely explanation is that the embrittling effect of hydrogen is eliminated because the dislocations introduced during warm working provide preferred sites (traps) for hydrogen atoms, thus preventing them from concentrating at grain boundaries where they result in premature failure due to intergranular fracture.

Fracture of annealed uranium containing sufficient concentrations of hydrogen has frequently been reported to occur intergranularly (Refs. 11, 17-18). While some of the fractographs in past reports have been of marginal clarity, unpublished fractographic observations by the authors clearly showed that the low ductility fracture surface of a salt annealed uranium sample was primarily intergranular with a small amount of cleavage and no evidence of microvoid coalescence (Ref. 19). This fracture surface was very similar to that shown in Figure 10b of Ref. 18, which corresponded to low ductility fracture. There is little doubt that the premature failure observed in Ref. 18 was caused by hydrogen embrittlement, since vacuum annealing greatly increased the material's ductility. The observations in Refs. 18 and 19 that hydrogen induced fracture occurs intergranularly strongly suggests that hydrogen concentration at the α-uranium grain boundaries is responsible for low ductility hydrogen assisted failure in annealed uranium.

The idea that hydrogen could be accumulating at grain boundaries and potentially forming UH_3 was suggested as early as 1956 by Davis (Ref. 20) and has continued to be discussed in the literature. Uranium hydride has been shown to sometimes form within the α-uranium grains or at grain boundaries in high hydrogen samples (Refs. 3, 17). Most recently, a paper by Harris, et. al., compared hydride volume fractions in cast vs. wrought uranium due to H-charging at 630°C followed by quenching. The authors measured hydride volume fractions utilizing small angle neutron scattering and observed that the cast material formed more hydride than the wrought material. The observed smaller volume fraction of uranium hydride in the wrought material was attributed to its much smaller grain size, and therefore higher grain boundary area, available to trap H (Ref. 21).

The idea of dislocations serving as H-traps in steel has been explored as early as 1980 by Krumnick, et. al. (Ref. 22) and more recently by Ha, et. al. (Ref. 23). They showed that higher amounts of hydrogen could be absorbed after significantly higher numbers of dislocations were introduced by cold working or plastic straining.

The feasibility of one weight ppm H concentrating at grain boundaries and causing embrittlement in annealed uranium, and the possibility that the increased dislocation densities typical of worked material could effectively trap this amount of hydrogen and overcome grain boundary embrittlement, was assessed as follows. Consider one cubic centimeter of α-uranium, which constitutes 0.0798 moles containing 4.81×10^{22} uranium atoms. One weight part per million hydrogen is equivalent to 238 atomic parts per million, so there would be $238 \times 10^{-6} \times 4.81 \times 10^{22} = 1.144 \times 10^{19}$ hydrogen atoms present.

If the one cm^3 cube was subdivided into 10 micrometer grains (the approximate grain size in the starting material of this study), roughly 3000 cm^2 of grain boundary area would be present. If the hydrogen atoms all concentrated on the grain boundaries there would be $1.144 \times 10^{19} / 3.0 \times 10^3 = 3.81 \times 10^{15}$ H atoms per cm^2 of grain boundary. The distance of closest approach of uranium atoms is 2.77×10^{-8} cm, so the approximate number of uranium atoms per cm^2 of grain boundary would be $\sim(2.77 \times 10^{-8})^{-2} = 1.30 \times 10^{15}$ U atoms/cm^2. Accordingly, the ratio of H atoms to U atoms on the grain boundaries would be approximately 3.81×10^{15} H atoms / 1.30×10^{15} U atoms = 2.93. This is essentially the stoichiometry of uranium hydride, UH_3. So if all the hydrogen atoms concentrated at the grain boundaries it would be reasonable to consider the grain boundaries as being potentially saturated with a monolayer of UH_3, which would almost certainly cause premature intergranular failure.

Typical dislocation densities in annealed metals are $\sim 1 \times 10^8$ cm/cm^3. If all the 1 wppm hydrogen atoms accumulated along these dislocations, there would be $1.144 \times 10^{19} / 1 \times 10^8 = 1.144 \times 10^{11}$ H atoms along every centimeter of dislocation line, or 1.144×10^3 H atoms per 10^{-8} cm – several orders of magnitude more H atoms than U atoms in the vicinity of each dislocation. The feasibility of such highly concentrated hydrogen atmospheres forming around dislocations is extremely low. This strongly suggests that the small numbers of dislocations in annealed material would be incapable of effectively trapping 1 wppm of hydrogen. But extensive dislocation multiplication occurs during plastic deformation, and the density of dislocations in material that has been significantly deformed is typically in the vicinity of $\sim 1 \times 10^{12}$ cm/cm^3. In this case there would be $1.144 \times 10^{19} / 1 \times 10^{12} = 1.144 \times 10^7$ H atoms along each centimeter of dislocation, and the mean spacing of H atoms would be $1 / 1.144 \times 10^7 = 8.7 \times 10^{-8}$ cm – roughly 3 times the distance of closest approach of the uranium atoms. Based on this, it seems entirely credible that the dislocations in warm worked material could potentially trap all of the hydrogen, thus dramatically reducing or eliminating H atom accumulation at the grain boundaries, and overcoming hydrogen embrittlement – exactly what has been experimentally observed in warm worked uranium.

The observation that plots of elongation and reduction-in-area vs. amount of warm deformation extrapolate to the values observed for hydrogen outgassed undeformed material (Figure 4) provides additional support for this proposal.

This approach also helps explain the effects of hydrogen content and loading rate on embrittlement of annealed uranium that have been reported by others (Refs. 12, 13). The most definitive studies of unalloyed uranium showed that tensile reductions-in-area for alpha-annealed samples tested at typical quasi-static rates gradually decreased from ~45% in hydrogen free samples to ~13% in samples containing 0.25 weight ppm hydrogen, then plateaued at ~13% at higher hydrogen contents (Refs. 12, 13). This information was reported for alpha-recrystallized material with a grain size of ASTM #7, equivalent to ~32 micrometer diameter. Calculations such as those presented above indicate that the U:H ratio corresponding to 0.25 wppm hydrogen and 32 micrometer grains would be 2.35. While this is a bit below the 3.0 value characteristic of UH_3, the difference is within the limits of these estimates. A U:H ratio of 3.0 would be obtained if grain size was increased to 41 micrometers (ASTM # 6.6, rather than 7), or the plateau in the ductility vs. H plot began at 0.31 ppm, rather than 0.25 – both are within the limits of the measurements reported in Refs. 12 and 13.

During testing at quasistatic rates, reduction in area was shown to decrease gradually as hydrogen concentrations increased from zero to 0.25 wppm (Refs 12, 13). But at much higher rates, reduction-in-area remained at ~45% for all H contents up to 0.25 wppm, then declined dramatically to 13% at 0.25 wppm H and higher. This suggests that at concentrations below 0.25 wppm the grain boundaries were less than fully saturated, and there was a need for additional hydrogen to be transported to the boundaries in the most critically stressed region in order for full embrittlement to occur. Such transport was apparently possible at low loading rates, resulting in the gradual decrease in ductility with increasing hydrogen content. But at high loading rates, insufficient time was available for hydrogen transport, so high ductility persisted up to the hydrogen content sufficient for grain boundary saturation without the need for additional transport during straining, i.e., hydrogen contents above 0.25 wppm.

A similar effect has been reported in U-0.75%Ti, where embrittlement in samples with as little as 0.06 wppm hydrogen occurred only at very low strain rates, but samples containing ~1 wppm hydrogen remained brittle at all strain rates (Ref. 24). The microstructure of quenched U-0.75%Ti is martensitic, so UH_3 formation and fracture occurred at the martensite plate boundaries, rather than at the α-grain boundaries of unalloyed uranium. This strain rate dependence at very low hydrogen contents and consistently low ductility at higher hydrogen contents supports the proposal that embrittlement occurs when boundaries become sufficiently saturated with hydrogen. And the observation that warm working of U-0.75%Ti helps eliminate fracture along the martensite plate boundaries, presented in Section 3.3, also supports the proposal that dislocations serve as traps for hydrogen in this alloy.

To further understand H interactions with various microstructural trap sites in a metal, thermal desorption spectroscopy (TDS) is often employed. Lillard and colleagues

conducted TDS on both single and polycrystalline α-uranium (Ref 25), in addition to powdered uranium hydride (Ref. 26) to identify major trap sites for H and estimate respective trapping energies. An extension of this technique that could confirm the hypotheses in the current work would be to use TDS to measure the amount of H desorbed from grain boundaries or dislocations compared to H desorbed from hydrides as a function of grain size or cold work. Using TDS to understand how much H above the solubility limit could be rendered innocuous by microstructural trapping could have important implications in a material that has such notoriously low solubility for H.

4.1.2. Directionality in Tensile Properties

The substantial differences between longitudinal and transverse properties are another significant feature that is apparent in Table 2 and Figures 3-6. Most notably, transverse ultimate strengths were markedly lower and transverse elongations markedly higher than their longitudinal counterparts. The combination of lower ultimate strength and higher elongation results from significantly lower strain hardening occurring in transverse tension than in longitudinal tension. This difference is believed to be due, at least in part, to preferred crystallographic orientation, or texture, as was described in Section 3.1.2

Rolling in the α-phase temperature range has previously been shown to result in substantial preferred crystallographic orientation, as summarized by Holden (Ref. 27) and confirmed by Teter, et. al. (Ref. 28). Typically (010) poles are preferentially located near the rolling direction and (100) poles near the transverse direction. Consistent with this, Smith and Ruckman have shown a strong tendency for (001) planes to increasingly align parallel to the surface in warm rolled uranium (Refs. 5, 28).

(010)[100] slip and (130) twinning are known to be the primary mechanisms by which room temperature plastic deformation occurs in α-uranium. However, the crystallographic nature of twinning makes its occurrence very sensitive to both orientation and sense of stress (tensile vs. compressive) in single crystals or textured polycrystalline samples. (130) twinning is known to occur primarily under the influence of compressive stress in the [010] direction or tensile stress in the [100] direction (Ref. 27). For the preferred orientation characteristic of warm rolled α-uranium, then, (130) twinning would be expected to be a major contributor to *transverse* tensile deformation, while (010)[100] slip would be the primary mode of *longitudinal* tensile deformation and a less important contributor to *transverse* tensile deformation.

Smith and Ruckman provided plots of how Schmid factors for (010)[100] slip and (130) twinning vary with stress axis for α-uranium grains in heavily warm rolled plate where the (001) planes were aligned parallel to the surface (Ref. 5). (Schmid factor = $\cos\phi \cos\lambda$, where ϕ = angle between stress axis and normal to plane on which deformation occurs, and λ = angle between stress axis and deformation direction.) High values of Schmid factor indicate high resolved shear stress on the deformation system in question, whereas low values indicate low resolved shear stress, therefore necessitating higher applied loads being required to initiate deformation.) For the idealized preferred orientation in which the [010] direction is perfectly parallel to the stress axis the Schmid factor for (010)[100]

slip in longitudinal tension would be zero ($\phi = 0°$ and $\lambda = 90°$). But taking into account the scatter that is typically inherent in preferred orientations, it is reasonable to estimate that, for longitudinal tension of heavily warm rolled uranium, Schmid factors for (010)[100] slip would range from 0 to ~0.2. These relatively low values indicate that resolved shear stresses would be low, so *longitudinal* tensile deformation by (010)[100] slip would be somewhat difficult.

Similar Schmid factors would be expected for (010)[100] slip in the *transverse* direction ($\phi = 90°$ and $\lambda = 0°$ for the idealized orientation), but considering scatter, values ranging from 0 to ~0.2 would again be reasonable However (130) twinning would be also be expected to be a major contributor to transverse tensile deformation. After (130) twinning begins the twinned material is significantly reoriented in a way that makes (010)[100] slip much easier within the twinned regions. Reflection of the (010) and [100] poles by the (130) twinning plane results in a Schmid factor of 0.34 for subsequent (010)[100] slip ($\phi = 68.8°$ and $\lambda = 21.2°$ for the idealized orientation). Considering scatter, values ranging from ~0.25 to ~0.4 are reasonable. The fact that this range of Schmid factors for (010)[100] slip in the twinned material are substantially higher than the 0 to ~0.2 range characteristic of the untwinned material indicates that, once twinning has commenced in *transverse* tension, (010)[100] slip will occur quite easily within the twinned material – more easily than in *longitudinal* tension where (130) twinning is not favored to occur. It is likely that this was a significant contributor to the lower strain hardening and higher ductility observed in *transverse* tension.

The preferred orientations of material that has been recrystallized after α-rolling have been shown to be very similar to those of the as-rolled material (prior to recrystallization) (Refs. 5, 27, 28). This explains why significant differences longitudinal and transverse tensile properties were observed even prior to warm rolling – the preferred orientations introduced during ingot breakdown were retained despite recrystallization having occurred during exposure to 630°C.

Obviously, if identical longitudinal and transverse properties are desired, the workpiece should be rotated between rolling passes in a way that minimizes in-plane crystallographic directionality. This has been investigated by others (Ref. 28)

4.2. U-2.3%Nb

The observation that previously annealed U-2.3%Nb becomes progressively more workable with increasing rolling temperature, particularly above ~200°C, results from multiple slip systems coming into play (Ref. 15), similar to what was observed in unalloyed uranium.

The addition of 2.3%Nb and the resulting change to a two-phase microstructure resulted in very significant increases in yield and ultimate tensile strength of the undeformed starting material relative to unalloyed uranium (increases of ~300 MPa in yield strength and 140 MPa in ultimate strength), with no accompanying decreases in elongation or reduction-in-area. No niobium was dissolved in the α-phase, so the increases in strength

were due to some combination of microstructural refinement (the characteristic lamellar spacing was ~2 micrometers, compared with ~10 micrometer grains in the unalloyed uranium), and the presence of the higher strength Nb-enriched γ-phase, likely containing ~12 wt.% Nb, and which evidence indicates is significantly harder and stronger than α-uranium (Ref. 29).

4.2.1. Effects of Rolling on Properties

The overall effects of cold and warm rolling on tensile properties, shown in Figures 8 to 17 and described in Section 3.2, were unsurprising. Rolling resulted in increases in yield and ultimate strength, and the magnitude of these increases decreased with increasing rolling temperature. Tensile ductility decreased with increasing strength. All these were consistent with expectations.

From an engineering perspective, rolling at temperatures below 200°C is impractical. Moderate increases in strength can be obtained by rolling at 265°C, but at the expense of significantly decreased elongation. Rolling at 375°C results in smaller increases in strength, but with substantially less reduction in ductility. Modest increases in strength can be obtained with heavy reductions at 500°C, without any significant ductility sacrifices.

Figures 8, 10, 12, and 14 show that compressive yield strength was frequently lower than tensile yield strength, particularly in conditions where relatively small reductions had been taken at low temperatures. The magnitude of these compressive-tensile differences decreased with increasing rolling temperature and at greater rolling reductions, and actually reversed at the highest rolling temperature, where compressive yield strengths exceeded those in tension, as can be seen in Figure 16.

4.2.2. Analysis of U-2.3% Nb Strengthening Components

This behavior led to consideration of several effects that contribute to tensile and compressive yield strengths: conventional strain hardening, the Bauschinger effect, and the effect of texture, i.e., preferred crystallographic orientation. These effects are illustrated in Figure 28 and described in equations 1-4:

$$TYS = \sigma_0 + LRD +/- BE/2 +/- TE/2 \quad \text{(eqs. 1\&2)}$$
$$CYS = \sigma_0 + LRD -/+ BE/2 -/+ TE/2$$

Where:
TYS = yield strength in tension,
CYS = yield strength in compression,
σ_0 = average of TYS & CYS prior to rolling,
LRD = long-range dislocation effect (conventional strain hardening),
BE = difference between TYS & CYS attributable to Bauschinger effect,
TE = difference between TYS & CYS attributable to texture effect.

Conventional strain hardening occurs because the extensive dislocation multiplication and interactions that occur during plastic deformation result in dislocation tangles and cell walls that serve as impediments to further dislocation movement. This component of strengthening, sometimes referred to as a long-range dislocation effect, is non-directional, i.e., it is unaffected by the sense of the strain (tensile vs. compressive). As a result, its magnitude can be determined from the average of tensile and compressive yield strength following a given amount of deformation, and how this compares with the value prior to deformation:

$$LRD = (TYS+CYS)/2 - (TYS_0+CYS_0)/2 \qquad \text{(eq. 3)}$$

Where:
TYS_0 and CYS_0 are the tensile and compressive yield strengths of the undeformed material, respectively.

The effects of rolling temperature and reduction on the long-range dislocation effect in U-2.3%Nb are shown in Figure 29. It can be seen that long-range dislocation strengthening increases with rolling reduction at all rolling temperatures. The magnitude of this effect decreases with increasing rolling temperature, but remains significant even with rolling at 500°C.

The Bauschinger effect and the texture effect are both directional and contribute to the difference between yield strengths in tension and compression.

The Bauschinger effect occurs when a metal that has previously been plastically deformed is unloaded and then deformed in the opposite sense, for example, first strained in compression, then unloaded and strained in tension. Yielding during reverse loading is frequently found to occur at a lower stress than the characteristic yield stress measured when the metal was originally loaded in the opposite sense. An example of this was described in the Introduction (Section 1), where hollow cylinders of U-0.75%Ti were compressively upset 1% to 3%. Compressive yield strengths were significantly increased as a result of upsetting, but tensile yield strengths remained virtually unchanged, due to the Bauschinger effect, as is illustrated in Figure 28.

The Bauschinger effect is a short-range dislocation phenomenon associated with dislocation pile ups that occur at obstacles during initial straining. The dislocation pile ups become progressively more concentrated as strain increases, and localized back stresses develop as the dislocations become more closely spaced. But when the sense of strain is reversed the dislocations begin to move in the opposite direction, i.e., dislocations move out of the pile ups and back stresses are relieved as the pile up concentrations decrease. Decreasing the pile up concentrations and relieving the associated back stresses occurs more easily than increasing them, so the yield stress in reversed straining is somewhat lower. Several detailed models have been developed for the Bauschinger effect (Ref. 30), but distinguishing between these is beyond the scope of this study.

Preferred crystallographic orientation, often referred to as texture, can also result in differences between tensile and compressive yielding and deformation in materials that deform by both slip and twinning, such as hexagonal close packed metals and alpha-uranium. Twinning is fundamentally a directional mechanism of deformation. Consideration of the crystallographic nature of twinning shows how twinning can occur or is prevented from occurring when single crystals of various orientations are strained in tension or compression (Ref. 31). This principle can be extended to polycrystalline metals with preferred crystallographic orientations, as was discussed in Section 4.1.2. A combination of slip and twinning are known to occur when compressive stresses are applied in the [010] direction α-uranium (Ref. 27). It is likely that the changes in preferred orientation that occur during rolling could alter the relative contributions of slip and twinning, thus affecting yield behavior in tension versus compression.

The Bauschinger and texture effects were both possible contributors to the tensile and compressive yield strengths of rolled U-2.3%Nb. The magnitude of these combined effects is given by:

$$BE + TE = (TYS\text{-}CYS)/2 - (TYS_0\text{-}CYS_0)/2 \qquad \text{(eq. 4)}$$

But since both effects are manifested in differences between tensile and compressive yield strength, it is not easy to separate them. In this study these effects were separated by identifying situations in which the Bauschinger effect was virtually certain to be zero, thus making the difference between tensile and compressive yield strength attributable only to texture. Plots of the texture effect versus deformation temperature and reduction were made based on data corresponding to these situations. The values of texture effect from these plots were then subtracted from the overall differences between tensile and compressive yield strength to determine how the Bauschinger effect varied with deformation temperature and reduction.

The undeformed fully annealed starting material is one case where the Bauschinger effect must be zero. Here the difference between tensile and compressive yield strengths, 630 MPa and 600 MPa, respectively, was 30 MPa, making the initial texture component 15 MPa. This relatively low value suggests that the starting material was not heavily textured. The absence of strong texture is consistent with the ingot of U-2.3%Nb having been broken down at 800° to 900°C in the γ-phase, where dynamic recrystallization occurred, and the γ-phase later diffusionally transforming to the $\alpha + \gamma$ microstructure shown in Figure 1.

Additional experiments were conducted to assess how the Bauschinger effect of previously rolled material was annealed out by exposure to elevated temperature. The Bauschinger component would be expected to anneal out at the lowest temperatures, since this involves only slight dislocation rearrangements. Annealing out of the long-range dislocation component should require somewhat higher annealing temperatures, as it involves much more significant reductions in dislocation density. The texture effect would be the most stable, not expected to anneal out until much more significant microstructural changes occurred, such as spheroidization and recrystallization of the

phases in the $\alpha + \gamma$ microstructure, or when the material was heated into higher temperature phase fields (>600°C).

The effects of annealing on tensile and compressive yield strengths, long-range dislocation strengthening, and the combined Bauschinger and texture effects are shown in Table 6. It can be seen that the long-range dislocation effect (the third row in Tables 6a and 6b) began to anneal out between 350° and 450°C for material previously rolled at both 25° and 265°C.

In material rolled at 25°C the combined Bauschinger and texture effects (rows 4 in Tables 6a and 6b) decreased significantly as annealing temperature increased to 350°C and then stabilized, indicating that the Bauschinger effect had been largely annealed out at 350°C. Based on this, the differences in tensile and compressive yield strength following annealing at 350°C and 450°C were attributed only to texture, indicating a texture effect of ~12 MPa. This is identical within experimental error to the 15 MPa value characteristic of the undeformed material, suggesting that no significant changes in texture occurred during room temperature rolling up to 20% reduction.

In contrast to this, annealing of material that had been previously reduced 67% at 265°C resulted in only minor changes in the combined Bauschinger and texture effects, even at the 450°C and 550°C temperatures where the long-range dislocation effect was significantly annealed out. This indicates that very little Bauschinger effect was present in the heavily deformed as-rolled material, and that the entire differences between tensile versus compressive yield strengths were attributable to texture effect, i.e., preferred orientation introduced during rolling.

These observations provided a partial basis for assessing how texture effect varied with rolling temperature and reduction. In addition, the differences between as-rolled tensile and compressive yield strengths in material that had been rolled at 500°C were taken to be due totally to texture effect, since the annealing studies indicated that the Bauschinger effect was annealed out at considerably lower temperatures.

Figure 30 shows a plot of how texture effect varied with rolling temperature and reduction. It can be seen that virtually no change in texture effect occurred during rolling at 25°C, but a modest change occurred during rolling at 265° and 500°C. Note that the texture effects corresponding to 67% reduction at 265°C and 70% reduction at 500°C are virtually identical. This implies that the lower line is applicable to all warm working temperatures, at least those between 265° and 500°C, and perhaps also 155°C where rolling behavior was much more like that at higher temperatures than at 25°C.

Figure 31 shows a plot of Bauschinger effect versus rolling temperature and reduction. Data for this plot was obtained by subtracting the texture effects shown in Figure 30 from the combined BE + TE values given by equation 4 for each rolled condition. It can be seen that a significant Bauschinger effect develops during initial rolling, then decreases at heavier reductions. The decrease at higher reductions likely occurs because increasingly dense dislocation tangles interfere with relaxation of dislocations from pileups during

reversed loading. Roughly equivalent Bauschinger effects occur during early rolling at 25°C and 265°C, but this decreases at higher rolling temperatures and goes to zero by 500°C. The peak effects shown at ~20% reduction are somewhat arbitrary, as compressive tests were conducted only at a few reductions – compressive yield strengths at intermediate reductions were estimated by interpolation. It can be said with certainty that relatively high Bauschinger effects occurred up to true strains of ~0.22 and were dramatically lower at true strains above 1.0, but the reductions corresponding to peak Bauschinger effect could not be determined with precision from this limited data set.

The overall result is that the increases in tensile and compressive yield strengths result from a combination of these effects. Comparison of Figures 29, 30, and 31 shows that the long-range dislocation effect contributes the most to deformation strengthening at all rolling temperatures. The Bauschinger effect is also significant, particularly at reductions up to ~20%. The texture effect is relatively small, even for high rolling reductions.

4.3. U-0.75%Ti

The observation that γ-quenched U-0.75%Ti is marginally workable at 25°C, but becomes much easier to roll at 250°C is similar to what was observed in unalloyed uranium and annealed U-2.3%Nb. Deformation mechanisms in the α'_b martensite are presumably similar to those in α-uranium, bringing multiple slip systems into play above ~200°C, and accounting for the relative ease of rolling at 250°C.

The yield strength of the quenched U-0.75%Ti starting material was ~70 MPa higher than that of annealed U-2.3%Nb and ~370 MPa higher than that of unalloyed uranium. It also exhibited equal or better tensile ductility than either vacuum annealed unalloyed uranium or U-2.3%Nb. This provided opportunities for even more impressive combinations of strength and ductility to be obtained by deformation strengthening of quenched U-0.75%Ti, or by a combination of deformation strengthening and age hardening, as will be discussed in Section 4.3.2.

4.3.1. Effects of Rolling on Tensile Properties

A substantial increase of ~300 MPa in tensile yield strength occurred in conjunction with the initial 10% reduction at 250°C, as shown in Figure 20. Additional rolling reductions produced more modest increases in yield strength. This is likely related to the combined effects of long-range dislocation strengthening and Bauschinger effect. Both components increase rapidly during initial deformation, but long-range dislocation strengthening later slows, and the Bauschinger effect peaks and then declines beyond ~10% deformation, as will be described in more detail in Section 4.3.3.

Ultimate tensile strength increased less dramatically during initial rolling, but continued to increase with further reduction, similar to what was observed in unalloyed uranium and U-2.3%Nb.

Figure 21 shows that elongation decreased with increasing amounts of 250°C rolling, but remained above 15% even at the high strength levels accomplished by extensive warm working. Reduction-in-area remained essentially unchanged at ~50% -- markedly different from the dramatic decreases that occur with conventionally age hardening (Ref. 26).

Table 7 provides a comparison of the properties obtained by warm working with those produced by conventional age hardening. It is apparent that deformation strengthened material exhibits consistently higher yield strengths, similar elongations, and dramatically higher reductions-in-area than material conventionally age hardened to the frequently specified ~900 MPa level of yield strength. Ultimate strengths are slightly lower for material warm worked 10% or 20%, but higher for material warm worked 50%. The last row of Table 7 shows that conventional aging to reach the ~1100 MPa yield strength level obtained in heavily warm worked material results in a severe sacrifice of ductility. So it is apparent that deformation strengthening provides superior combinations of strength and ductility in almost all ways.

Macroscopic fracture morphology and microscopic fracture surface appearance confirm that excellent ductility is retained in deformation strengthened material, as summarized in Table 4. Tensile samples of material heavily rolled at 250°C continued to exhibit cup-and-cone fractures with substantial shear lips, similar to those of the very ductile as-quenched samples. Microscopically, failure continued to occur primarily by microvoid coalescence, albeit with slightly finer dimples.

The retention of very high reduction-in-area, significant shear lips, and microvoid coalescence in deformation strengthened material are dramatically different from what is observed in conventionally age hardened material. Age hardening typically results in substantial decreases in reduction-in-area, the virtual elimination of shear lips, and a transition to quasi-cleavage fracture along martensite plate boundaries, as shown in Table 4.

The marked differences in fracture behavior associated with deformation strengthening versus conventional age hardening may be related to hydrogen effects. It is known that hydrogen embrittlement of U-0.75%Ti can result in dramatic reductions in ductility and a transition from microvoid coalescence to quasi-cleavage along martensite plate boundaries (Ref. 24). Hydrogen contents of ~1 wppm are sufficient to cause embrittlement at all strain rates. Embrittlement can occur even at extraordinarily low hydrogen concentrations (e,g., 0.06 wppm) if strain rates are low enough to permit transport of hydrogen to triaxially stressed regions.

Very similar reductions in ductility and a transition to quasi-cleavage fracture are characteristic of age hardening in U-0.75%Ti, as can be seen by comparing Figures 24 and 25. Metals typically become more susceptible to hydrogen embrittlement as their strength increases. So it is possible that the quasi-cleavage fracture observed in age hardened U-0.75%Ti alloys is, at least in part, associated with increased sensitivity to hydrogen – even at concentrations below 0.2 wppm.

However, if strengthening is accomplished by deformation, rather than aging, the dislocations introduced by warm working could serve as traps for hydrogen atoms. This would make the deformation strengthened material more tolerant of hydrogen, similar to what was observed with unalloyed uranium. Ductility would remain relatively high and quasi-cleavage failure would be avoided. These are exactly what have been observed in deformation strengthened U-0.75%Ti, as shown in Tables 4 and 7.

4.3.2. Aging After Warm Working

The results of preliminary tests done to screen the effects of deformation and subsequent aging on hardness are shown in Figure 18. The hardening effects of deformation and aging are initially additive – prior deformation does not accelerate age hardening at 380°C, nor does aging at 380°C reduce the hardening effects of prior deformation. But at higher aging temperatures this is no longer true. The hardening imparted by prior deformation begins to be annealed out, resulting in a dynamic balance between age hardening and annealing. Figure 18 shows that at 420°C the offsetting effects of age hardening and annealing out of deformation hardening result in a hardness plateau at ~Rc 49. Presumably aging at slightly lower temperatures would result in this balance beginning at higher deformation amounts, for example at ~20% reduction for aging at 400°C, and at ~50% reduction for aging at 380°C.

This trend is apparent in the tensile property plots shown in Figures 22 and 23. The data corresponding to 0% deformation show the substantial effects of conventional age hardening at 380°C and 400°C on both strength and ductility. But less aging-related strengthening occurs after 20% warm working, and nearly none after 50% warm working.

Regarding strength, material previously warm rolled 20% exhibited aging-related increases in yield and ultimate strength, reflecting a continuing dominance of age hardening over annealing out of earlier deformation effects. But in material previously rolled to 50% reduction, subsequent aging resulted in virtually no further increases in strength. This indicated that age hardening and annealing were effectively balanced against one another. Even here, however, the yield and ultimate strengths of heavily worked plus age hardened samples were higher than those produced by age hardening alone, confirming that the deformation effect had not been fully annealed out, and that a combination of deformation strengthening and age hardening was responsible for the observed strengths.

Figure 23 shows that aging of material that had been rolled 20% at 250°C resulted in significant decreases in elongation and reduction-in-area, but markedly less than those that occurred on comparable aging of previously undeformed material. Material that had been rolled 50% prior to aging exhibited essentially no age-related decrease in elongation and only a modest decrease in reduction-in-area. This suggests that the benefits in fracture behavior imparted by earlier high deformation were largely retained throughout aging.

Fractographic evidence supports this, as indicated in Table 4. Conventional aging resulted in quasi-cleavage failure, as shown in Figure 25. But material that had been lightly deformed prior to aging fractured by mixed quasi-cleavage and microvoid coalescence, as shown in Figure 26. And material that had been heavily deformed prior to aging failed totally by microvoid coalescence, as shown in Figure 27. This suggests that sufficient numbers of dislocations remained from deformation to effectively trap hydrogen.

From an engineering perspective, the decreases in ductility that resulted from subsequent age hardening of previously deformation strengthened material outweighed the small increases in strength. The best combinations of tensile yield strength and ductility were obtained in material that had been deformation strengthened only.

4.3.3. Analysis of U-0.75%Ti Strengthening Components

Two proprietary data sets containing tensile and compressive property information from deformation strengthened U-0.75%Ti cylinders were provided to the authors for the purpose of analyzing the components contributing to deformation strengthening (Refs. 8, 34). Both involved deformation by compressive upsetting, as was described in Section 1. Upsetting was done at 25°C, 300°C, and 350°C. Both data sets also included samples that had been age hardened at 375°C or 380°C, mostly after upsetting. Good ductility (tensile elongations greater than 20%) was characteristic of all conditions, except for a few samples that failed prematurely at obvious defects.

The components of strengthening were analyzed using equations 1-4. But in this case σ_0 included the strengthening effect of age hardening, estimated from other work to be approximately 200 MPa (Ref. 32). Material prior to upsetting exhibited somewhat higher yield strengths in compression than tension (differences of ~130 (Ref. 8) and ~165 MPa (Ref. 34), respectively). This indicated that the extensive hot working done during fabrication of the starting cylinders resulted in significant preferred orientation and texture effect – much greater than were characteristic of the U-2.3%Nb plates, where less hot work had been done during ingot breakdown. Cylinder upsetting was assumed to produce negligible changes in the texture effect, as the relatively small deformations done during upsetting were deemed unlikely to significantly alter the preferred orientations introduced during the much more extensive fabrication processes.

The effects of deformation amount and temperatures on long-range dislocation strengthening are shown in Figures 32 and 33. Figure 32 shows that identical results were obtained regardless of whether aging was done before or after deformation. This confirms that room temperature deformation and aging at 380°C were additive, at least up to 20% compressive reduction, as had been inferred from the earlier hardness results (Figure 18). Figure 33 shows that the magnitude of long-range dislocation strengthening rises most rapidly during early deformation. Increases continue with further deformation, but at progressively decreasing rates. Significantly less long-range dislocation strengthening occurs during deformation at 300°C and 350°C than at 25°C, as expected.

Figures 34 and 35 show the effects of deformation temperature and subsequent aging on the Bauschinger effect. The magnitude of the Bauschinger effect increases rapidly during initial deformation, peaks at ~10% deformation, then decreases with further deformation, similar to what was seen in U-2.3%Nb (Figure 31). Figure 34 shows that significantly greater Bauschinger effect occurred in material that was aged prior to deformation, indicating that 380°C aging after deformation decreased the Bauschinger magnitude somewhat. The Bauschinger magnitude also decreased with increasing deformation temperature, as shown in Figure 35. This is again similar to the trend observed in U-2.3%Nb.

Comparison of Figures 32 and 34 shows that the magnitude of the Bauschinger effect was comparable to that of long-range dislocation strengthening, particularly when age hardening was done prior to 25°C upsetting. The directional Bauschinger effect contributed positively to compressive yield strength, resulting in compressive yield strengths as high as ~1500 MPa. The Bauschinger effect facilitated earlier yielding in tension, making the corresponding tensile yield strengths only ~750 MPa. However ultimate tensile strengths were ~1350 MPa, only slightly lower than the ~1425 MPa value for conventionally age hardened material, and tensile elongations exceeded 25%, slightly better than those of conventionally aged material.

Additional data obtained for swaged U-0.75%Ti (Ref. 14) confirmed the importance of the Bauschinger effect. Material that had been swaged at 250°C to 58% area reduction (true strain of 0.868) exhibited tensile yield strength of 1200 MPa, 400 MPa higher than the compressive yield strength of 800 MPa. Even greater effects were seen when the final swaging pass was done at 25°C. Swaging resulted in higher axial yield strength in tension than in compression (opposite to that in compressively upset material) because the swaging process compressed the material radially, thus increasing the length of the workpiece – similar to straining in axial tension. As a result, the Bauschinger effect contributed positively to tensile yield strength and detracted from compressive yield strength in swaged material.

Additional data for U-0.75%Ti bars that had been rotary straightened (Ref. 14) could also be understood in terms of long-range dislocation strengthening and the Bauschinger effect. Rotary straightening involved repeated cycles of tensile and compressive straining at room temperature with estimated strain magnitudes in the vicinity of 1% to 3%. This resulted in similar increases in tensile and compressive yield strength – both in the vicinity of 140 MPa. The Bauschinger effect was near zero because the strains imposed by straightening were both tensile and compressive. Hence, the similar increases in both tensile and compressive yield strength were due primarily to the long-range dislocation strengthening introduced during straightening. Figure 32 confirms that strains as low as those typical of rotary straightening result in long-range dislocation strengthening magnitudes consistent with those observed in rotary straightened material.

4.3.4. Further Comments on Properties of Warm Rolled U-0.75%Ti Plate

The above results suggest that the high longitudinal tensile yield strengths for warm rolled U-0.75%Ti plate described in Sections 3.3 and 4.3.1 were due to a combination of long-range dislocation strengthening and the Bauschinger effect. It is likely that longitudinal compressive yield strengths (which were not measured) would be considerably lower due to the opposite sense of the Bauschinger effect in material whose length had been increased by rolling, rather than decreased by axial compression.

In warm rolled then aged U-0.75%Ti the offsetting balance between deformation strengthening and age hardening described in Sections 3.3 and 4.3.2 likely occurred due to the Bauschinger effect being gradually annealed out during aging at 380°C or higher. While such aging heat treatments resulted in relaxation of dislocation pile ups, the high density of tangled dislocations responsible for long range dislocation strengthening remained. These dislocations likely provided trapping sites for hydrogen, thus enabling much higher ductility than in conventionally age hardened material which had not been previously warm worked.

4.4 General Discussion and Synthesis

Several commonalities are apparent across the alloys and types of deformation investigated.

First, deformation provided for increased ductility. In the case of unalloyed uranium this was associated with overcoming the embrittling effects of hydrogen, likely because the numerous dislocations introduced by warm working served as trapping sites for hydrogen atoms, preventing their concentrating at grain boundaries and causing brittle intergranular fracture. A similar but more subtle effect occurred in U-0.75%Ti, where hydrogen related quasi-cleavage fracture along martensite plate boundaries was avoided when material was strengthened by deformation rather than conventional aging. Warm rolling resulted in significantly better combinations of tensile yield strength and ductility, with fracture occurring by microvoid coalescence. Warm rolling prior to aging also helped overcome quasi-cleavage fracture, again suggesting that dislocations provided traps for hydrogen.

Second, deformation resulted in significant directionality in properties. In heavily warm rolled unalloyed uranium this took the form of differences in longitudinal and transverse strain hardening associated, at least in part, with the preferred orientation introduced by rolling. In previously annealed U-2.3%Nb and previously quenched U-0.75%Ti it was manifested as difference between tensile and compressive yield strengths associated mostly with the Bauschinger effect.

Third, analysis of the components of deformation strengthening showed that the Bauschinger effect contributed strongly during initial deformation, but peaked and later decreased with higher amounts of deformation, particularly during exposure to moderately elevated temperature, either during or following deformation. Long-range dislocation strengthening also occurred most rapidly during initial deformation, but continued to increase indefinitely with increasing deformation. Long-range dislocation strengthening was less affected by subsequent exposure to moderately elevated temperatures than Bauschinger strengthening

Finally, from the perspective of metal fabrication, processes such as rolling are only practical at temperatures above ~200°C, at least when 25.4 cm diameter rolls are used. But modest amounts of deformation can be done at room temperature by other methods, such as compressive upsetting or swaging. All of these result in a substantial Bauschinger effect, which can be exploited to tailor tensile and compressive properties to specific engineering applications.

5. Conclusions

Warm rolling of unalloyed uranium produces superior combinations of strength and ductility due to a combination of deformation strengthening and overcoming of the embrittling effects of hydrogen. Dislocations introduced during deformation likely serve as hydrogen trapping sites, preventing hydrogen from concentrating at grain boundaries and causing intergranular fracture. Large differences in longitudinal and transverse properties result, at least in part, from preferred crystallographic orientation introduced during unidirectional rolling.

The addition of 2.3%Nb results in a 2-phase microstructure with substantially higher initial strength. Warm rolling results in a combination of long-range dislocation strengthening and a Bauschinger effect. The Bauschinger effect causes differences between yield strength in tension and compression.

Solution treated and quenched U-0.75%Ti can be deformation strengthened to provide significantly better combinations of yield strength and ductility than can be obtained by conventional age hardening. Long-range dislocation strengthening and the Bauschinger effect are both significant contributors. Subsequent aging results in offsetting age hardening and annealing out of the Bauschinger effect, but good ductility is retained.

Acknowledgements

This report summaries the results obtained in collaborative efforts at several institutions supported by the U. S. Departments of Energy and Defense. Compilation, analysis, and documentation of these efforts was supported by Los Alamos National Laboratory, with the particular encouragement of Paul Dunn. Samantha Lawrence provided helpful conversations and suggestions.

References

1. K. H. Eckelmeyer, "Uranium and Uranium Alloys", ASM Metals Handbook, 10th Ed., Vol. 2, Properties and Selection, 1991, pp. 670-682.
2. J. Boulton and P. D. Tilbury, "The Influence of Warm Rolling Upon the Ductile/Brittle Transition Temperature of α-Uranium", J. Inst. Metals, Vol. 92, 1963, p. 93.
3. D. M. Taplin and J. W. Martin, "The Effect of Grain Size and Cold Work On the Tensile Properties of Alpha-Uranium", J. Less Common Metals, Vol. 7, 1964, pp. 89-97.
4. N. Hughes, R. A. Lane, and S. Orman, "The Effects of Warm Work On Some Mechanical and Fabrication Properties of Uranium", J. Nucl. Mat'ls. Vol. 48, 1973, pp. 172-182.
5. C. J. E. Smith and J. C. Ruckman, "The Effect of Warm Working on the Microstructure and Ductility of Uranium", AWRE O 27/70, 1970.
6. A. M. Ammons, "Precipitation Hardening in Uranium-rich Uranium-Titanium Alloys", in Physical Metallurgy of Uranium Alloys, J. J. Burke, et. al., Eds, Brook Hill, 1976, pp. 511-585.
7. S. W. Zehr, "The Mechanical Properties of Two-Phase Uranium Alloy, in Physical Metallurgy of Uranium Alloys, J. J. Burke, et. al., Eds, Brook Hill, 1976, pp. 393-424.
8. E. L. Bird, Y-12 National Security Center, Unpublished Research, 1990
9. J. L. Cadden, N. C. Jessen, and P. S. Lewis, "Melting and Casting of Uranium Alloys", in Physical Metallurgy of Uranium Alloys, J. J. Burke, et. al. Editors, Brook Hill, 1976, pp. 3-81.
10. W. L. Owen, "Effect of Hydrogen on Mechanical Properties of Uranium", Metallurgica, 1962, pp. 3-6.
11. A. N. Hughes, S. Orman, and G. Picton, "The Embrittlement of U By H_2O and Hydrogen", Corrosion Science, Vol. 10, 1970, pp. 239-244.
12. G. L. Powell and J. B. Condon, "Hydrogen in Uranium Alloys", in Physical Metallurgy of Uranium Alloys, J. J. Burke, et. al., Eds, Brook Hill, 1976, pp. 427-461.
13. G. L. Powell, Overview of Hydrogen Embrittlement of Uranium and Uranium Alloys", in Metallurgical Technology of Uranium and Uranium Alloys, ASM, 1982, pp. 877-899.
14. G. B. Dudder, Pacific Northwest National Laboratory, Unpublished Research, 1988.
15. J. S. Daniel, B. Lesage, and P. Lacombe, "The Influence of Temperature on Slip and Twinning in Uranium", Acta Met., Vol. 19, 1971, pp. 163-173.
16. S. K. Lawrence, Los Alamos National Laboratory, Private Communication, 2020.
17. P. Adamson, S. Orman, and G, Picton, "The Effects of Hydrogen on the Tensile Properties of Uranium When Tested in Different Environments", J. Nucl. Matls., Vol. 33, 1969, pp. 215-224.
18. J. Huddart and P. A. Bleasdale, "The Effect of Strain Rate on the Tensile Flow and Fracture of α-Uranium", J. Nucl. Matls., Vol. 89, 1980, pp. 316-330.
19. P. Tubesing and K. H. Eckelmeyer, Los Alamos National Laboratory, Unpublished Research, 2002.

20. Davis, W. D., “Solubility, Determination, Diffusion and Mechanical Effects of Hydrogen in Uranium”, Knolls Atomic Power Lab, KAPL-1548, 1956.
21. Harris, Z., Garlea, E., Boyd, T., DeBeer-Schmitt, L., Littrell, L. K., Agnew, S., “Assessing the Influence of Microstructure on Uranium Hydride Size Distributions via Small Angle Neutron Scattering, Materialia, Vol. 28, 2023.
22. Kumnick, A. J., Johnson, H. H., “Deep Trapping States for Hydrogen in Deformed Iron”, Acta Met., Vol. 28, 1980, pp. 33-39.
23. Ha, H. M., Ai, J-H., Scully, J. R. “Effects of Prior Cold Work on Hydrogen Trapping and Diffusion in API X-70 Line Pipe Steel During Electrochemical Charging”, Corrosion, 70 (2), 2014, pp. 166–184.
24. B. C. Odegard Jr., K. H. Eckelmeyer, and J. J. Dillon, “The Embrittement of U-0.8% Ti By Absorbed Hydrogen”, in Hydrogen Effects on Material Behavior, N. R. Moody and A. W. Thompson, eds., TMS, 1990.
25. Lillard, R. S., and Forsyth, R. T., "A Thermal Desorption Spectroscopy Study of Hydrogen Trapping in Polycrystalline α-Uranium." J. Nucl. Mat’ls., Vol. 461, 2015, pp. 341-349.
26. Lillard, R. S., et al. "A Thermal Desorption Study of the Kinetics of Uranium Hydride Decomposition." J. Nucl. Mat’ls., Vol. 444, 2014, pp. 49-55.
27. N. Holden, Physical Metallurgy of Uranium, Addison-Wesley, 1958, pp. 78-118.
28. D. F. Teter, et. al., “Processing-Property Relationships in Wrought Uranium”, LA-UR-06-2890, 2006.
29. K. H. Eckelmeyer, A. D. Romig, Jr., and L. J. Weirick, “Quench Rate Effects in U-6%Nb”, Metallurgical Transactions, Vol. 15A, 1984, pp. 1319-1330.
30. P. S. Bate and D. V. Wilson, “Analysis of the Bauschinger Effect”, Acta Met. Vol. 34, 1986, pp. 1097-1105.
31. R. W. Hertzberg, Deformation and Fracture of Engineering Materials, John Wiley, 1976, pp. 101-114.
32. K. H. Eckelmeyer and F. J. Zanner, “The Effect of Age Hardening on the Mechanical Behavior of U-0.75 wt.%Ti and U-2.0wt.%Mo”, J. Nucl. Mat’ls. Vol 62, 1976, pp. 37-49.
33. K. H. Eckelmeyer, A. D. Romig, Jr., G. M. Ludtka, G. Mackiewicz-Ludtka, and L. R. Chapman, “The Effect of Ti Content on Age Hardening and Mechanical Properties of Uranium-Titanium Alloys”, J. Nucl. Mat’ls., Vol. 562, 2022, pp. 1-28.
34. W. T. Nachtrab, Nuclear Metals Inc., Unpublished Research, 1989.

Table 1. Compositions of materials studied
(in weight percent or weight parts per million)

Element	Unalloyed Uranium (a)	U-2.3%Nb	U-0.8%Ti
Nb	-	2.27%	-
Ti	-	< 10 ppm	0.81%
C	100 ppm (max)	59 ppm	30 ppm
Al	15 ppm (max)	5 ppm	5 ppm
Ca	50 ppm (max)	< 2 ppm	< 10 ppm
Fe	75 ppm (max)	10 ppm	30 ppm
Mg	5 ppm (max)	< 2 ppm	3 ppm
Ni	50 ppm (max)	4 ppm	9 ppm
H	(b)	(c)	(c)

a) Chemical analyses not available. Numbers represent typical specification for vacuum induction melted material produced by this process.
b) Hydrogen content of material which has been heated to 630°C in molten salt is typically 1 to 2 ppm H.
c) Hydrogen content of U-2.3%Nb and U-0.8Ti plates are expected to be ~0.1 to 0.2 ppm following vacuum annealing at 800°C for 4 hours.

Table 2. Effects of processing on tensile properties of unalloyed uranium.

a) Longitudinal properties:

Rolling Reduction (%)	Finish Temp. (°C)	Vac. Anneal (°C/hrs)	Grain Shape	H Content (wppm)	YS (MPa)	UTS (MPa)	Elong (%)	RA (%)
60	350	630/0.5 (in salt)	Equiaxed	1-2	345	840	8	8
60	350	630/2	Equiaxed	< 0.2	325	915	24	39
60	350	None	Elongated	1-2	405	1005	24	38
60	350	300/24*	Elongated	< 0.2	405	1015	26	43
60	250	None	Elongated	1-2	570	1170	20	40
93.5	250	None	Elongated	1-2	730	1350	18	50

b) Transverse properties:

Rolling Reduction (%)	Finish Temp. (°C)	Vac. Anneal (°C/hrs)	Grain Shape	H Content (wppm)	YS (MPa)	UTS (MPa)	Elong (%)	RA (%)
60	350	630/0.5 (in salt)	Equiaxed	1-2	345	580	5	5
60	350	630/2	Equiaxed	< 0.2	340	785	40	60
60	350	None	Elongated	1-2	495	895	33	47
60	350	300/24*	Elongated	< 0.2	510	905	35	53
60	250	None	Elongated	1-2	600	970	34	54
93.5	250	None	Elongated	1-2	690	1040	35	55

(*): Removes H, but does not recrystallize material – elongated grains and dislocation structure introduced by rolling remain.

Table 3. Comparison of Longitudinal and Transverse Tensile Properties
In Deformation Strengthened U-0.75%Ti

Processing	Orientation	Yield Strength (MPa)	Ultimate Strength (MPa)	Elongation (%)	Reduction In Area (%)
Rolled 10% at 250°C	Longitudinal	1031	1407	23	49
"	Transverse	923	1380	24	48
Rolled 50% at 250°C	Longitudinal	1120	1680	17	50.5
"	Transverse	1075	1596	20	51.5

Table 4. Effect of Processing on Fracture Morphology and Fracture Surface Appearance of U-0.75%Ti

Reduction At 250°C (%)	Aging (°C/hrs)	Reduction In Area (%)	Shear Lip (% of fracture surface)	Shear Lip Fracture Appearance	Center Region Fracture Appearance
0	None	51	75	Coarse dimples (~10-15μm)	Coarse dimples (~6-10 μm)
10	None	49	65	Coarse dimples (~10-15μm)	Coarse dimples (~6-10 μm)
50	None	50.5	60	Slightly finer dimples (~8-12 μm)	Slightly finer dimples (~5-8 μm)
None	400/5	22	<5	Fine dimples (~4-6 μm)	Quasi-cleavage
10	400/5	37	30	Midsized dimples (~6-8 μm)	Quasi-cleavage & fine dimples (~3-6 μm)
50	400/5	42.5	40	Very fine dimples (~2-3 μm)	Very fine dimples (~1-5 μm)

Table 5. Comparison of tensile properties of warm rolled & vacuum annealed unalloyed uranium.

Processing	H Content (wppm)	Orientation	Yield Strength (MPa)	Ultimate Strength (MPa)	Elongation (%)	Reduction In Area (%)
Annealed at 630°C (a)	< 0.2	Longitudinal	325	915	24	39
Rolled 60% Finishing at 250°C (b)	1-2	Longitudinal	570	1170	20	40
Annealed at 630°C (a)	< 0.2	Transverse	340	785	40	60
Rolled 60% Finishing at 250°C (b)	1-2	Transverse	600	970	34	54

a) Annealed in vacuum to reduce hydrogen content to less than ~0.2 weight ppm.
b) Warm worked samples had been heated to 630°C in molten salt in preparation for rolling, resulting in hydrogen contents in the vicinity of 1 to 2 weight ppm.

Table 6. Effect of annealing temperature on properties of previously rolled U-2.3%Nb (annealed 5 hours).

Previously rolled at 25°C to 20% reduction:

	As-rolled	150°C	250°C	350°C	450°C	550°C
TYS (a) (MPa)	879	855	854	854	751	-
CYS (b) (MPa)	732	725	772	827	730	-
LRD (c) (MPa)	190	175	198	226	126	-
BE+TE (d) (MPa)	74	65	41	14	10	-

Previously rolled at 265°C to 67% reduction:

	As-rolled	150°C	250°C	350°C	450°C	550°C
TYS (a) (MPa)	876	-	-	868	757	710
CYS (b) (MPa)	888	-	-	912	808	743
LRD (c) (MPa)	267	-	-	275	168	112
BE+TE (d) (MPa)	-6	-	-	-22	-26	-16

a) Tensile yield strength
b) Compressive yield strength
c) Long-range dislocation effect: LRD = (TYS+CYS)/2 - (TYS_0+CYS_0)/2, where (TYS_0+CYS_0)/2 refers to the unworked starting material = 615 MPa
d) BE+TE = (TYS-CYS)/2 – (TYS_0-CYS_0)/2, where (TYS_0-CYS_0)/2 refers to the unworked starting material = 15 MPa

Table 7. Comparison of U-0.75%Ti Tensile Properties Produced By Conventional Aging Versus Deformation Strengthening.

Processing	Yield Strength (MPa)	Ultimate Strength (MPa)	Elongation (%)	Reduction In Area (%)
Solution Treated (no aging, no rolling)	703	1324	31	51
Conventionally Aged 400°C/5 hrs	922	1517	20	22.5
Rolled 10% at 250°C (0.105 True Strain)	1031	1407	23	49
Rolled 20% at 250°C (0.223 True Strain)	1048	1478	20	49
Rolled 35% at 250°C (0.431 True Strain)	1111	1525	18	50.5
Rolled 50% at 250°C (0.693 True Strain)	1120	1680	17	50.5
Conventionally Aged 455°C/2 hrs (a)	1110	1620	5	5

a) Aged to obtain yield strength equivalent to that of material rolled 35% or 50% at 250°C.

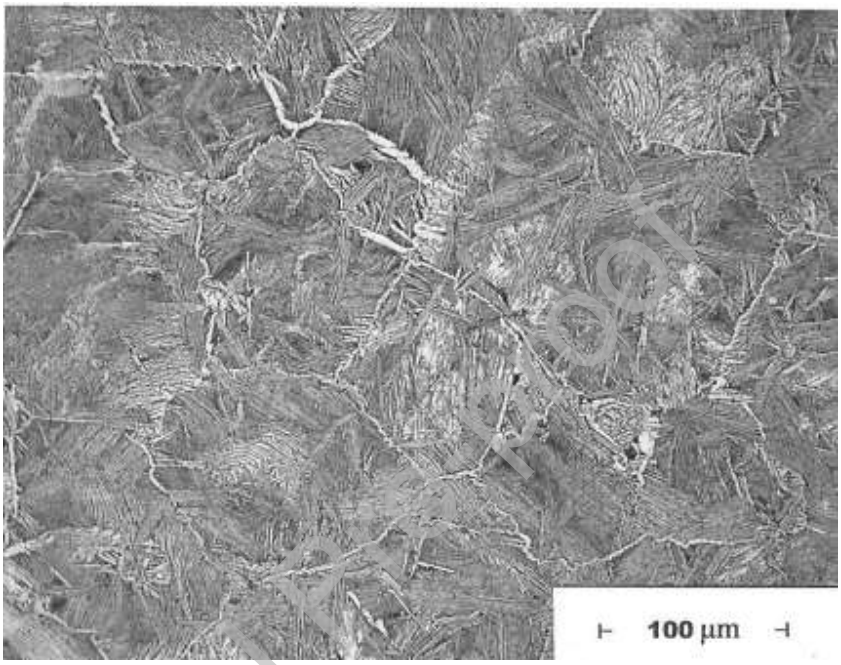

Figure 1. Microstructure of U-2.3% Nb starting material. Vacuum annealed at 800°C and furnace cooled. Prior-γ grain boundaries are decorated with thin layer of α-phase and grain interiors exhibit 2-phase lamellar α-phase + Nb-enriched γ-phase resulting from monotectoid decomposition.

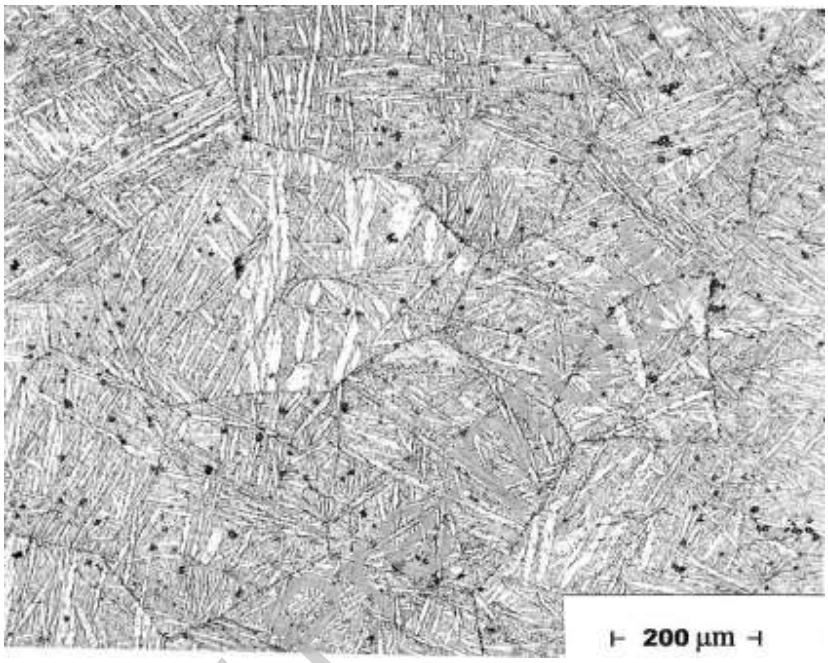

Figure 2. Microstructure of U-0.75%Ti starting material. Vacuum annealed at 800°C and water quenched. Microstructure consists of ~200 μm prior-γ grains transformed primarily to α'_a acicular martensite (bright lenticular features) with some diffusionally transformed $\alpha + U_2Ti$ microconstituent in the interstices between the martensite plates (gray microconstituent, individual phases too fine to be resolved).

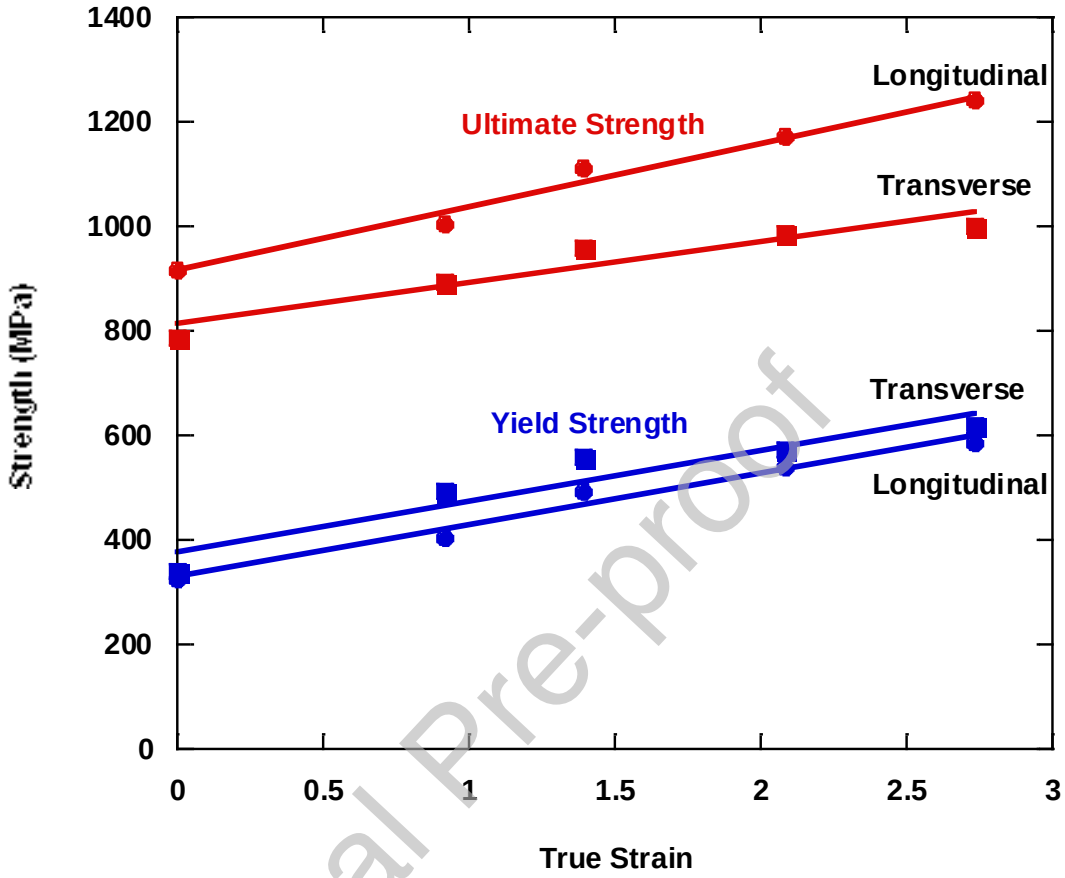

Figure 3. Effect of 350°C rolling reduction on yield and ultimate strengths of unalloyed uranium (tested at 25°C). Data points represent rolling reductions of 0%, 60%, 75%, 87.5%, and 93.5%, equivalent to true strains of 0, 0.916, 1.386.2/079, and 2.733, respectively. Lines represent best fit linear correlations.

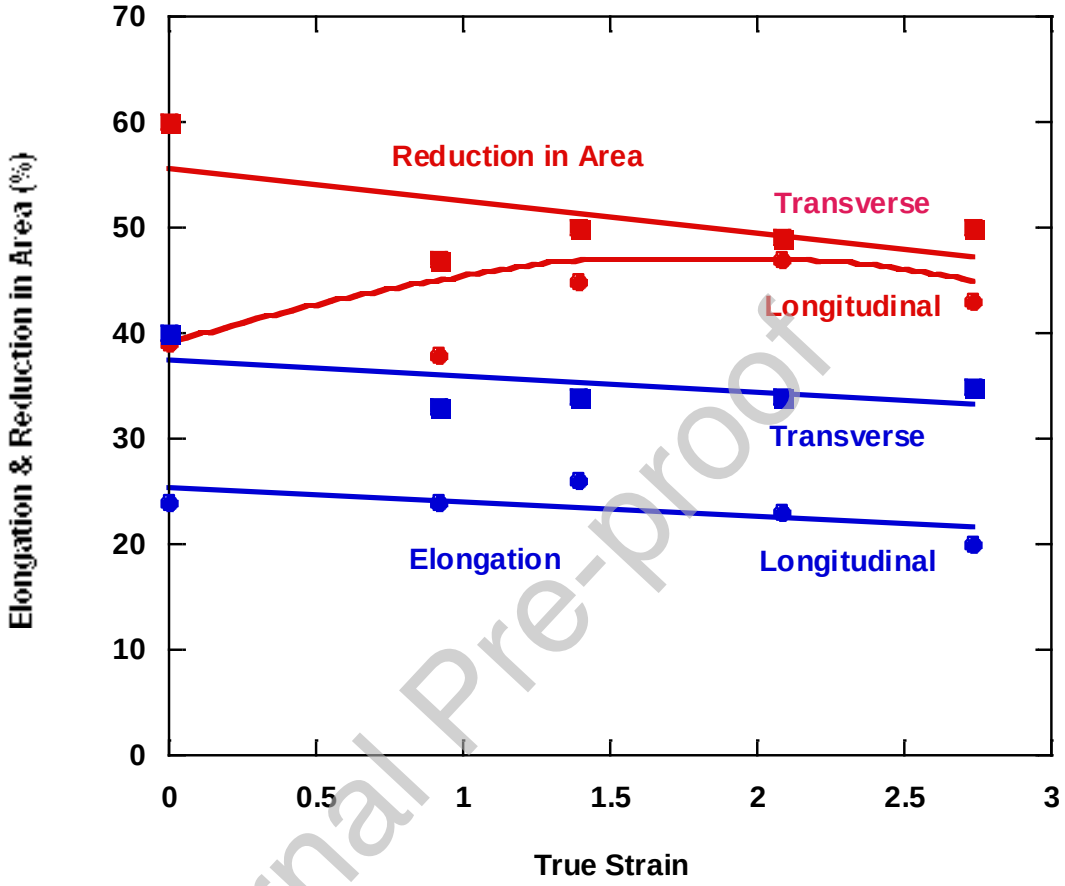

Figure 4. Effect of 350°C rolling reduction on elongation and reduction-in-area of unalloyed uranium (tested at 25°C). Data for 0 strain (unworked material) corresponds to material that had been vacuum annealed at 630°C; the ductility of material that had been annealed in molten salt was dramatically lower (see Table 2). All data for warm worked conditions corresponds to material that had been heated to 630°C in molten salt in preparation for warm rolling. Lines represent best fit linear correlations.

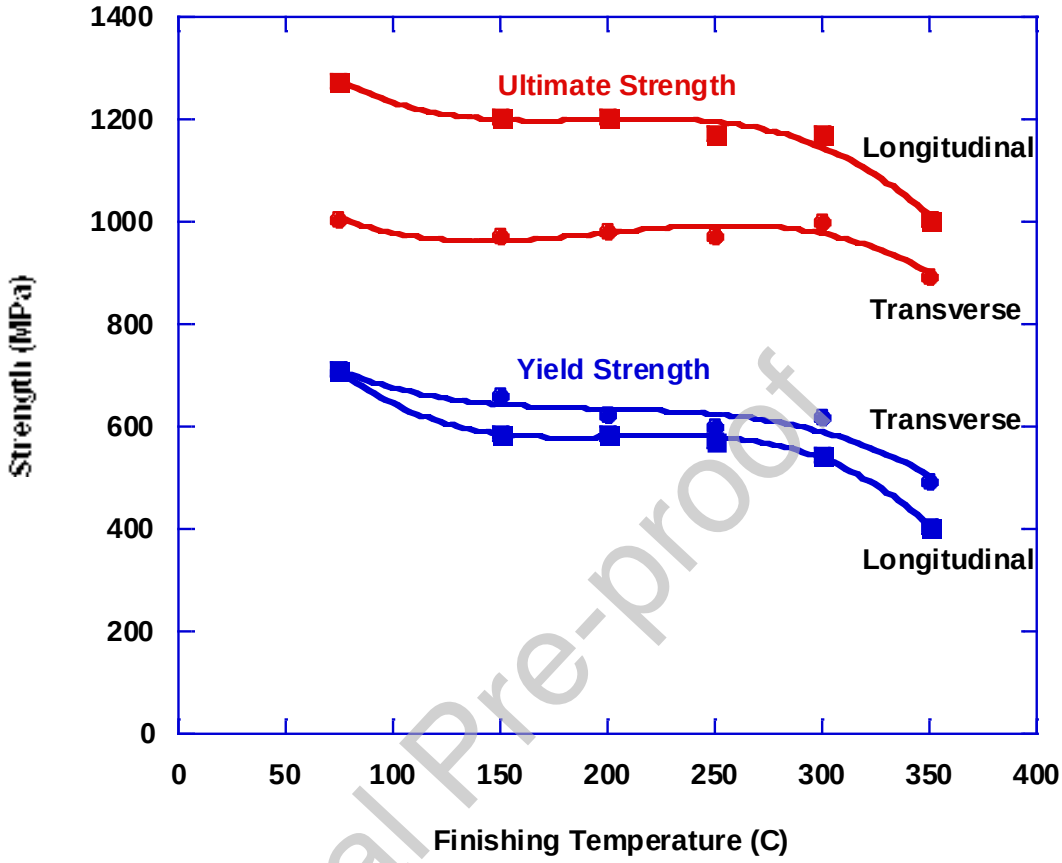

Figure 5. Effect of finishing temperature on yield and ultimate strength of unalloyed uranium (tested at 25°C). All samples rolled to 60% reduction (true strain = 0.916).

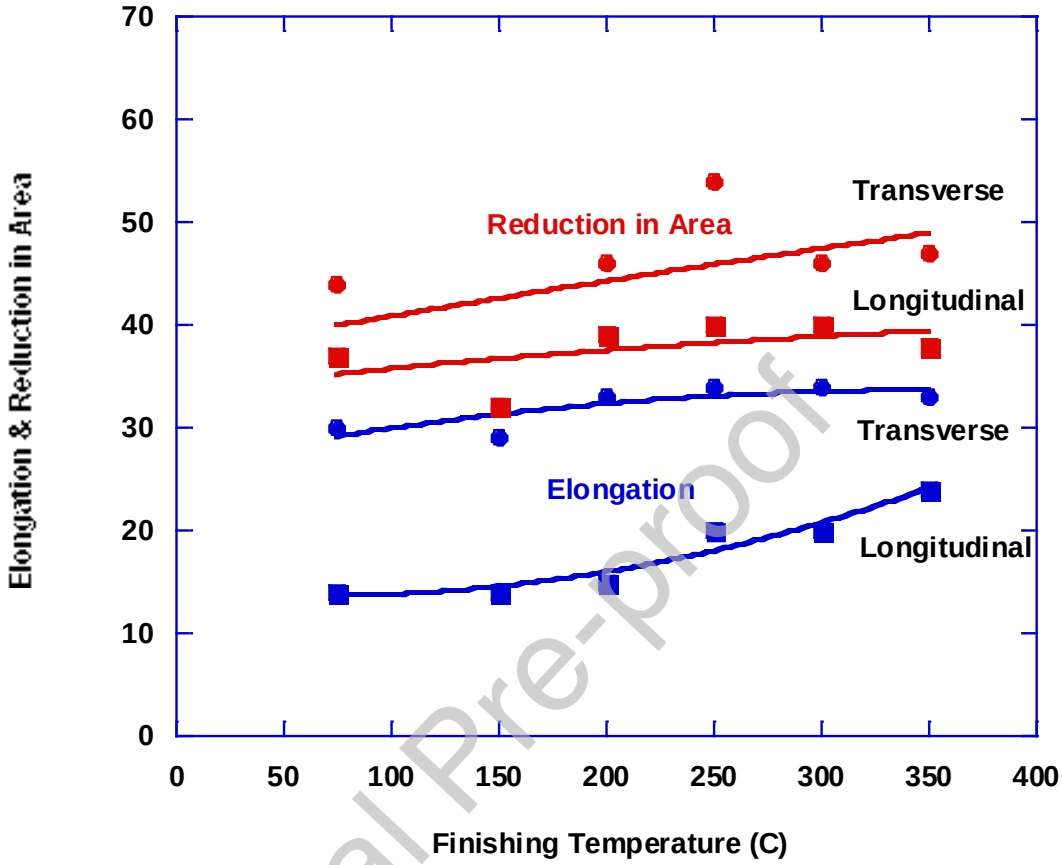

Figure 6. Effect of finishing temperature on elongation and reduction-in-area of unalloyed uranium (tested at 25°C). All samples rolled to 60% reduction (true strain = 0.916). All data corresponds to material that had been heated to 630°C in molten salt in preparation for warm rolling.

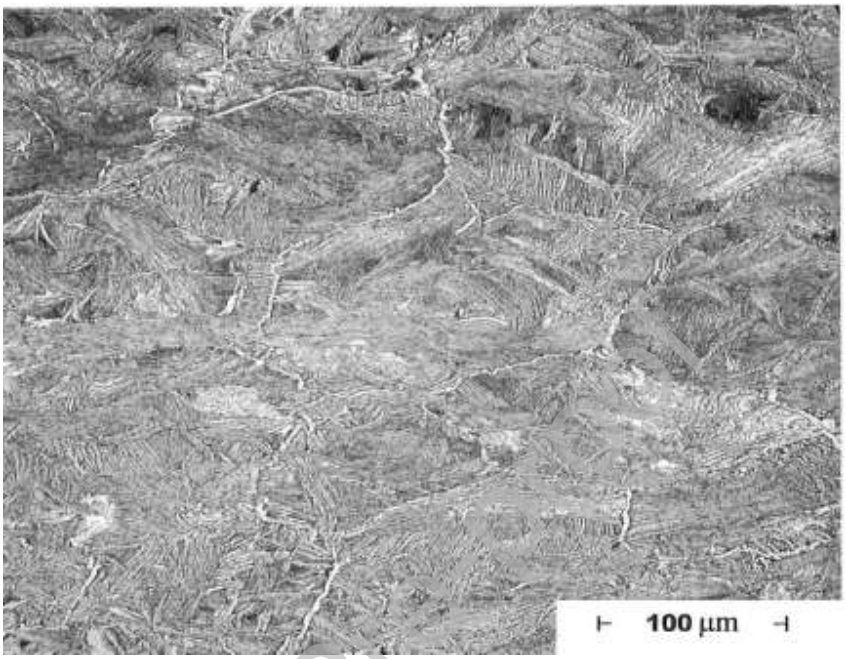

Figure 7. U-2.3% Nb rolled to 40% reduction (true strain = 0.51) at 265°C.

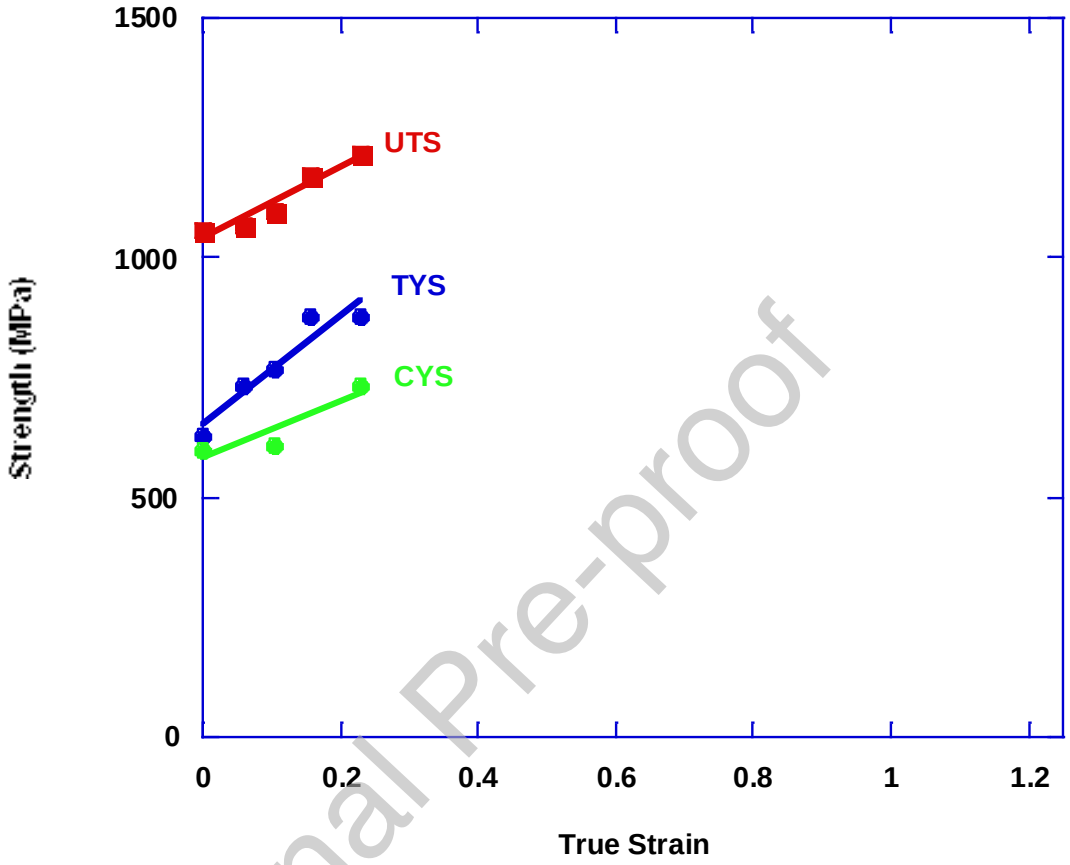

Figure 8. Effect of rolling at 25°C on tensile and compressive yield strengths and ultimate tensile strength of U-2.3%Nb.

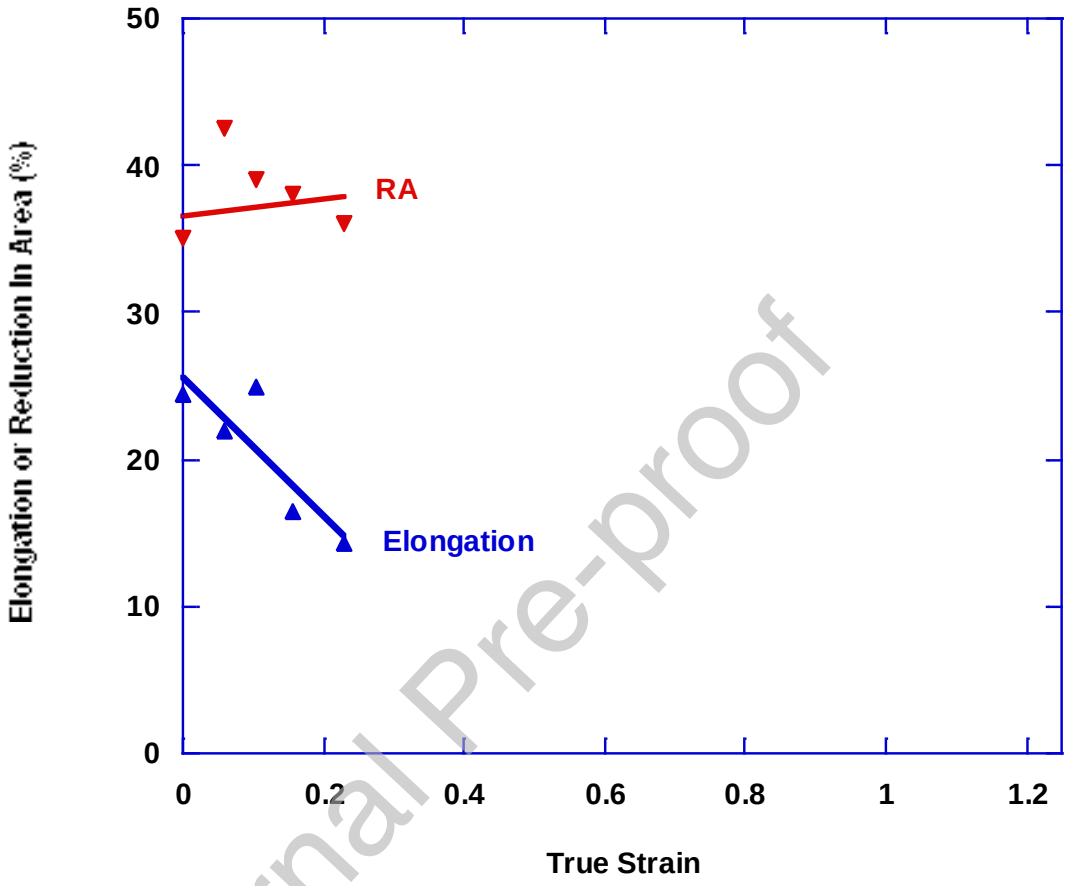

Figure 9. Effect of rolling at 25°C on ductility of U-2.3%Nb.

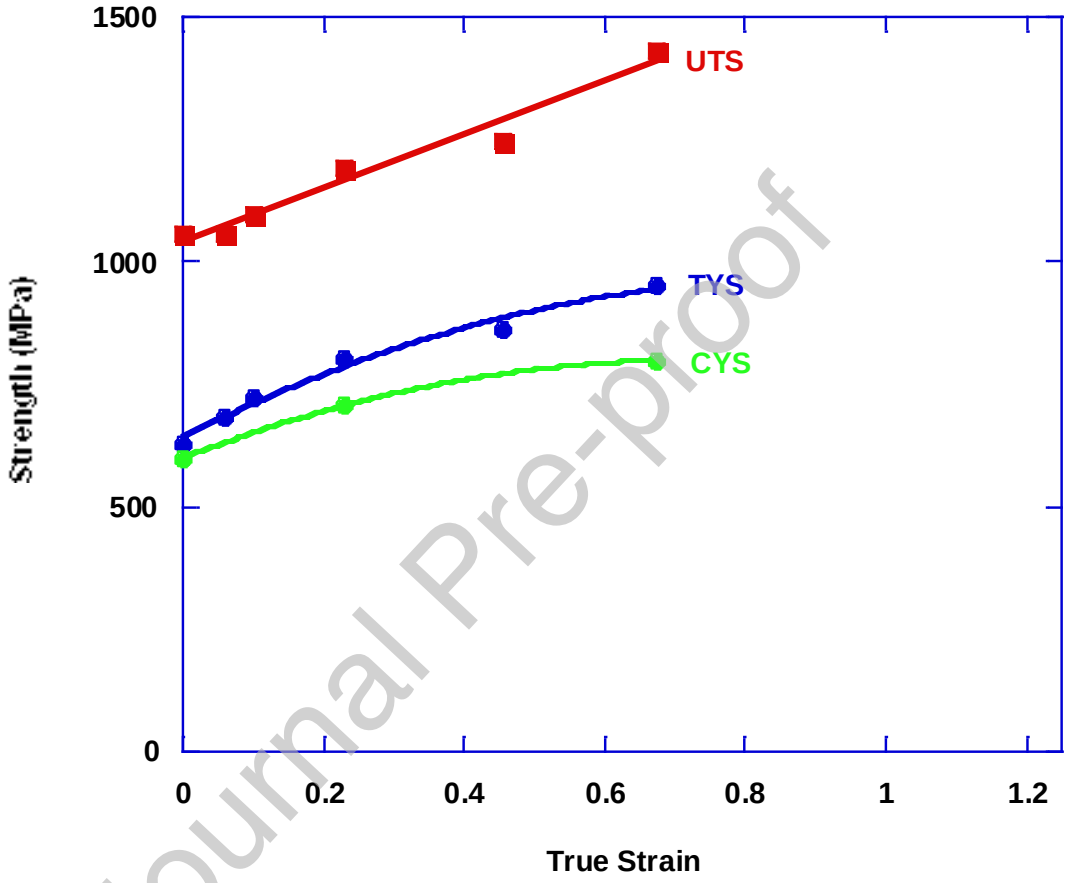

Figure 10. Effect of rolling at 155°C on tensile and compressive yield strengths and ultimate tensile strength of U-2.3%Nb.

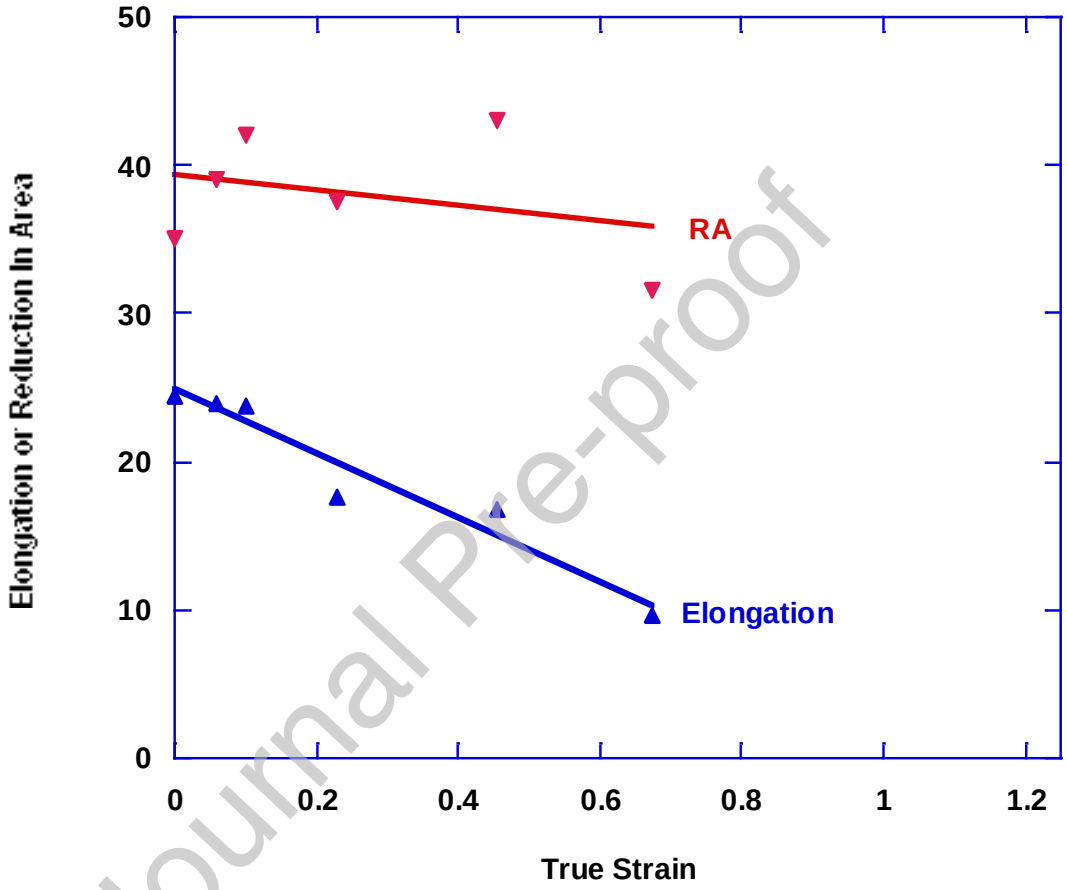

Figure 11. Effect of rolling at 155°C on ductility of U-2.3%Nb.

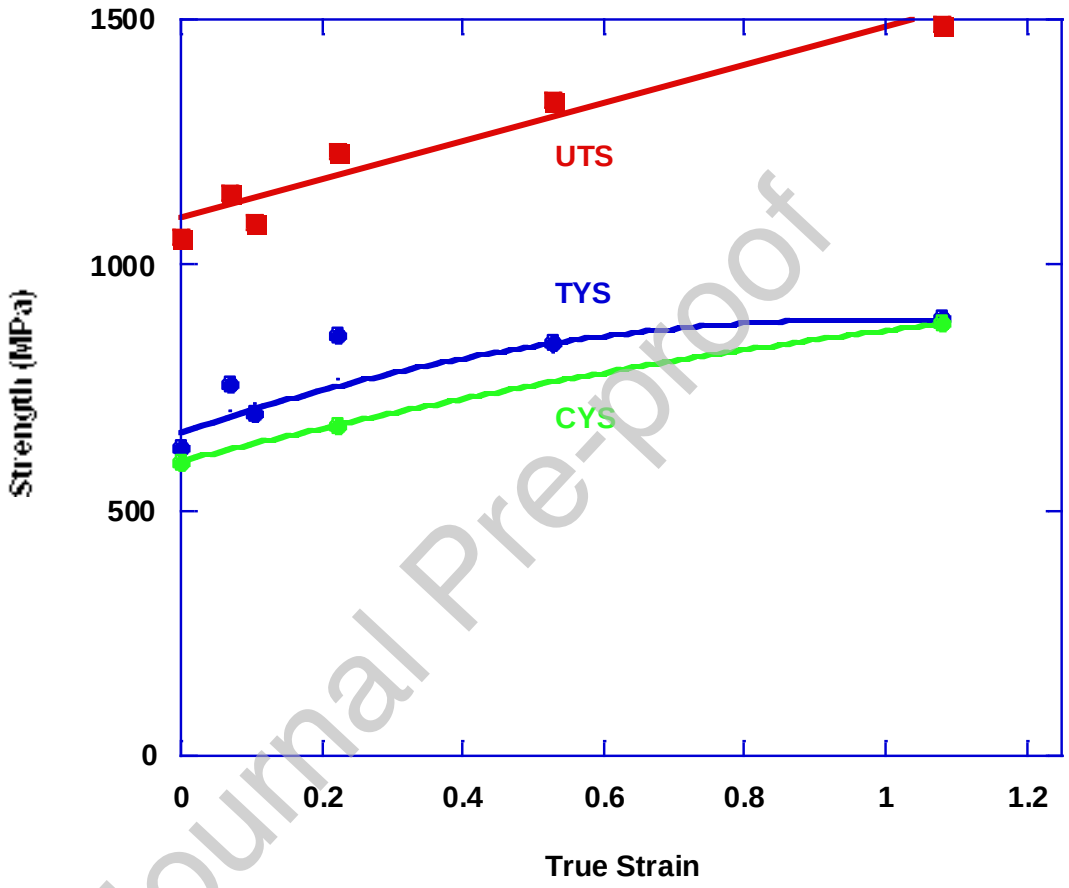

Figure 12. Effect of rolling at 265°C on tensile and compressive yield strengths and ultimate tensile strength of U-2.3%Nb.

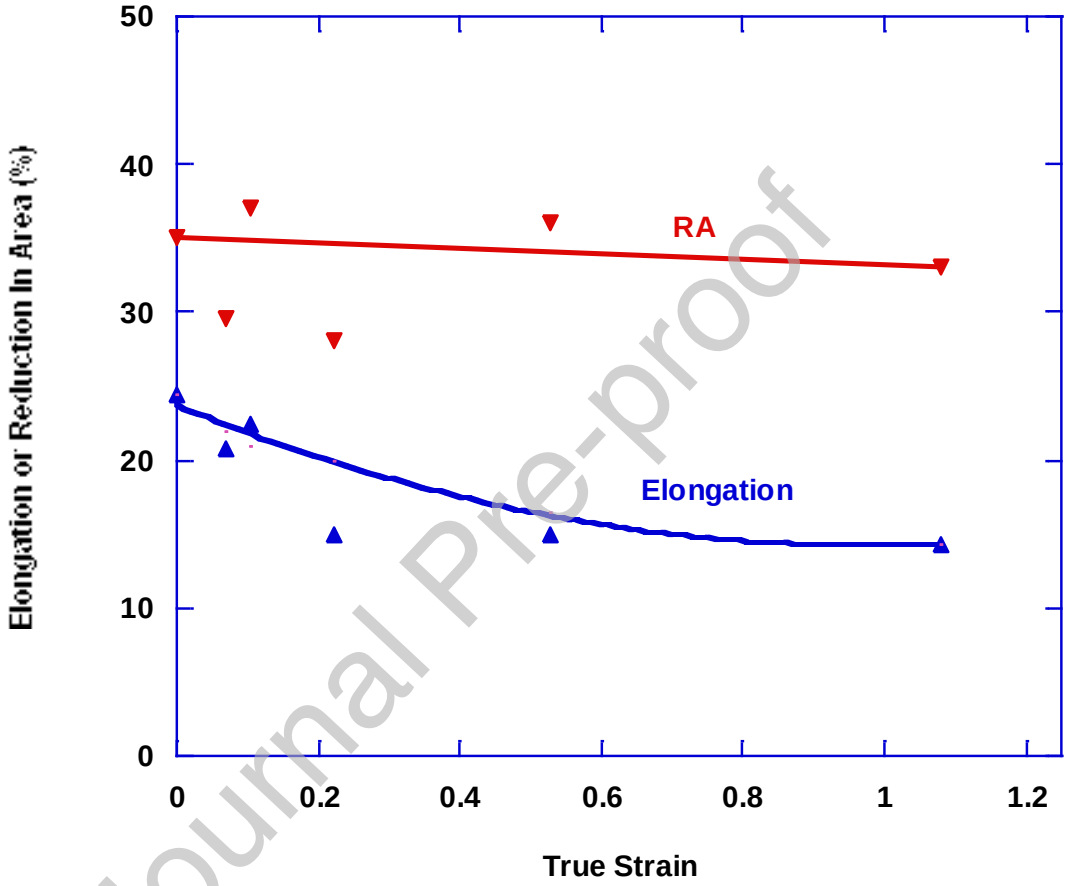

Figure 13. Effect of rolling at 265°C on ductility of U-2.3%Nb.

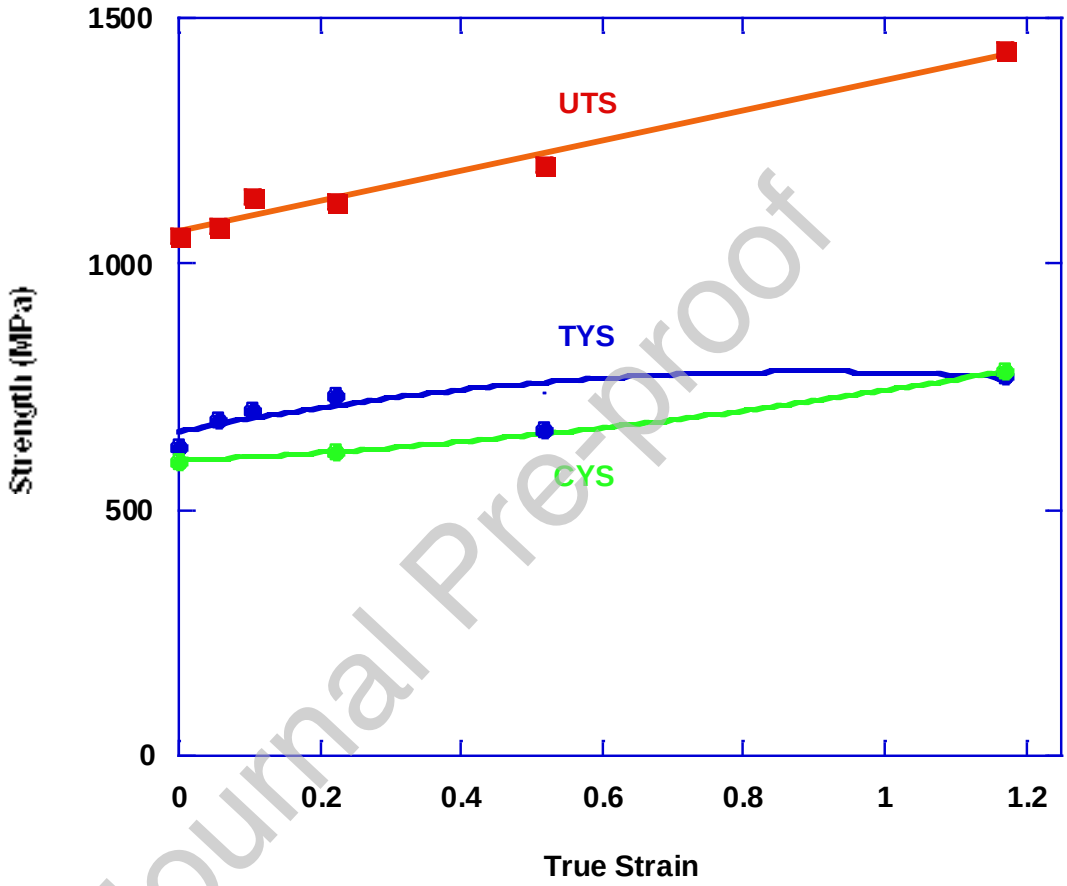

Figure 14. Effect of rolling at 375°C on tensile and compressive yield strengths and ultimate tensile strength of U-2.3%Nb.

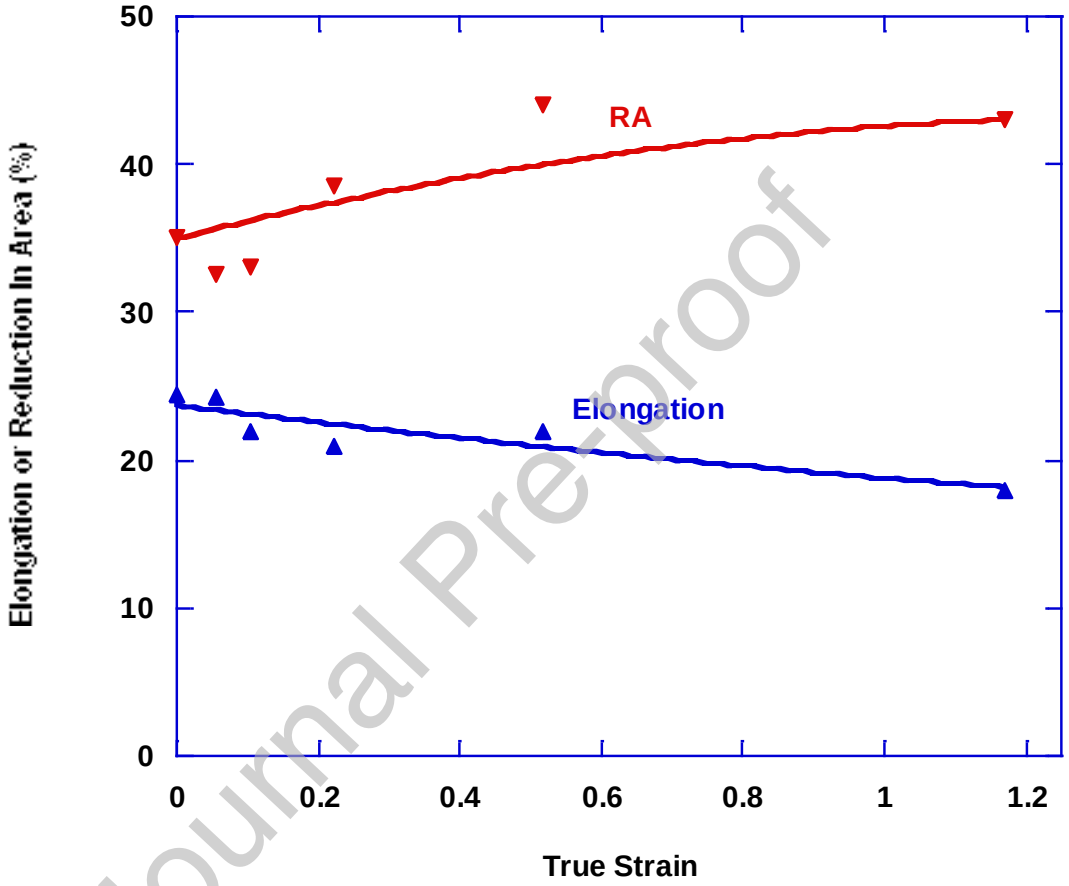

Figure 15. Effect of rolling at 375°C on ductility of U-2.3%Nb.

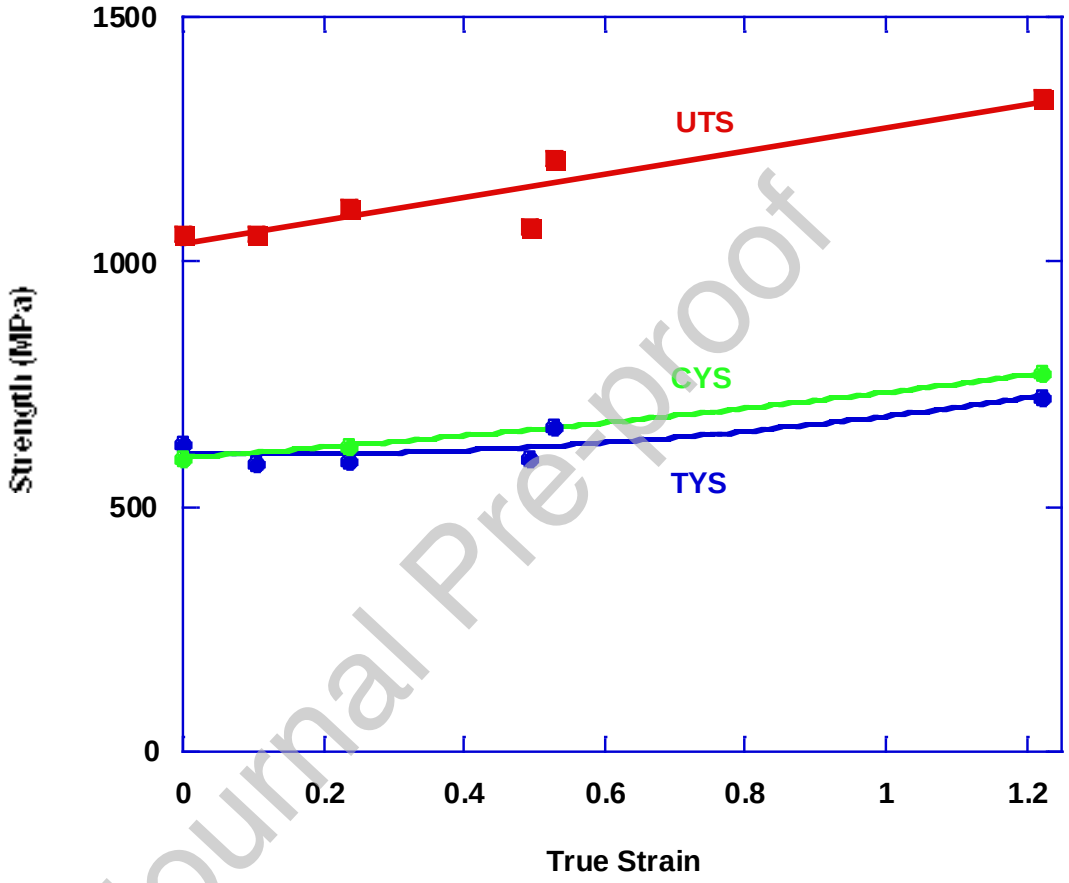

Figure 16. Effect of rolling at 500°C on tensile and compressive yield strengths and ultimate tensile strength of U-2.3%Nb.

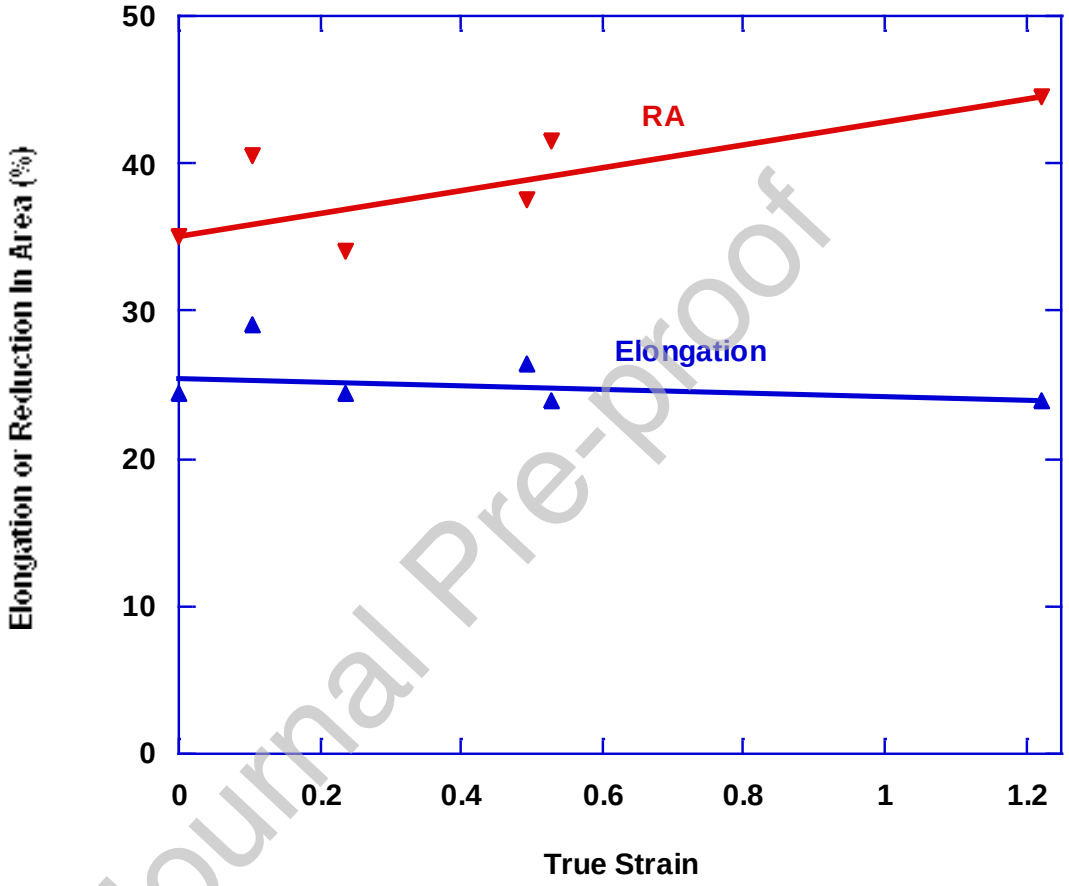

Figure 17. Effect of rolling at 500°C on ductility of U-2.3%Nb.

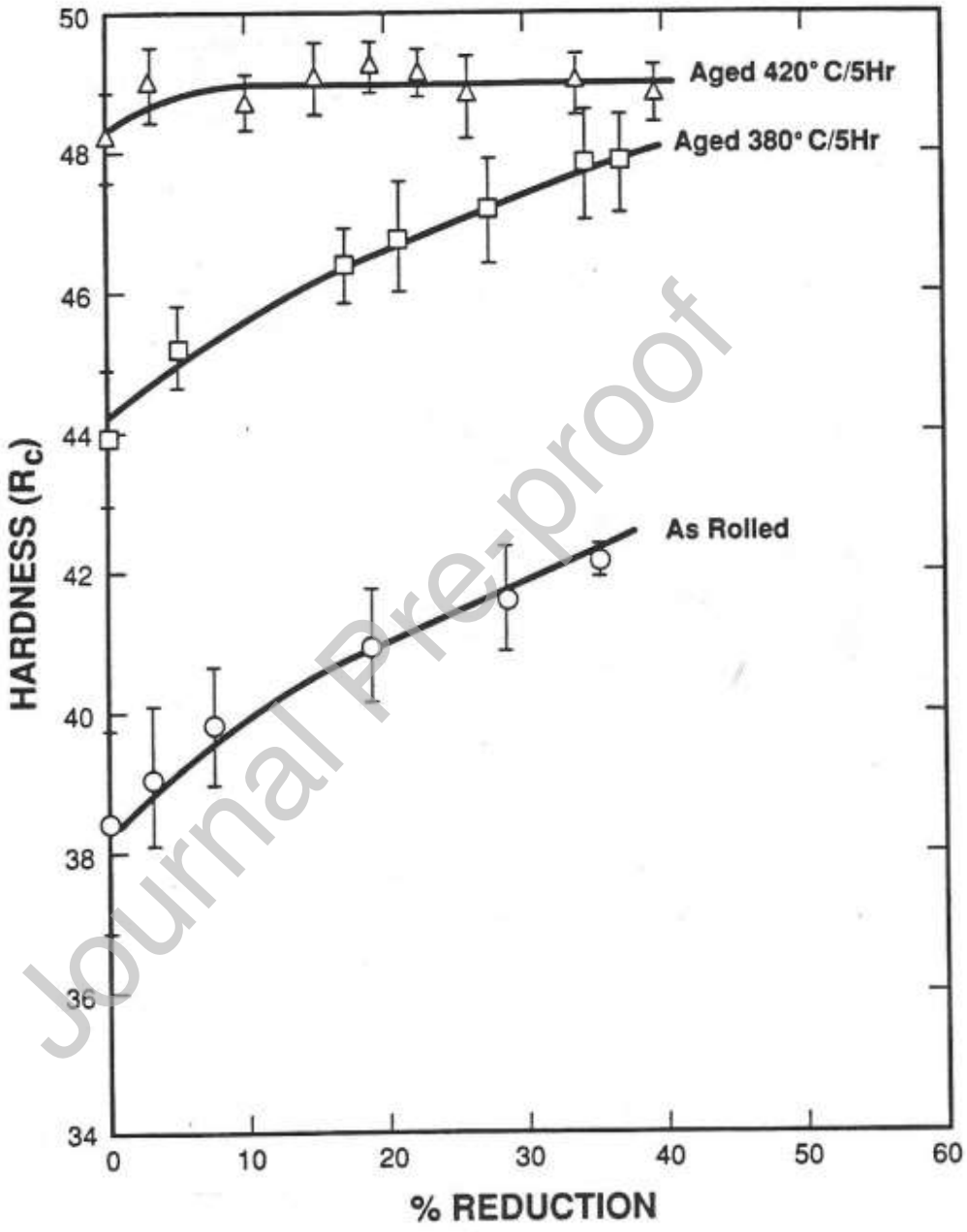

Figure 18. Effect of rolling and subsequent aging on hardness of U-0.75%Ti. Error bars represent 95% confidence limits from at least 5 hardness tests at each location. Conventional aging at 380°C for 5 hours corresponds to fractional hardening of ~0.4 (40% of peak aged hardness or yield strength). Conventional aging at 420°C for 5 hours corresponds to fractional hardening of ~0.8. (Ref. 33).

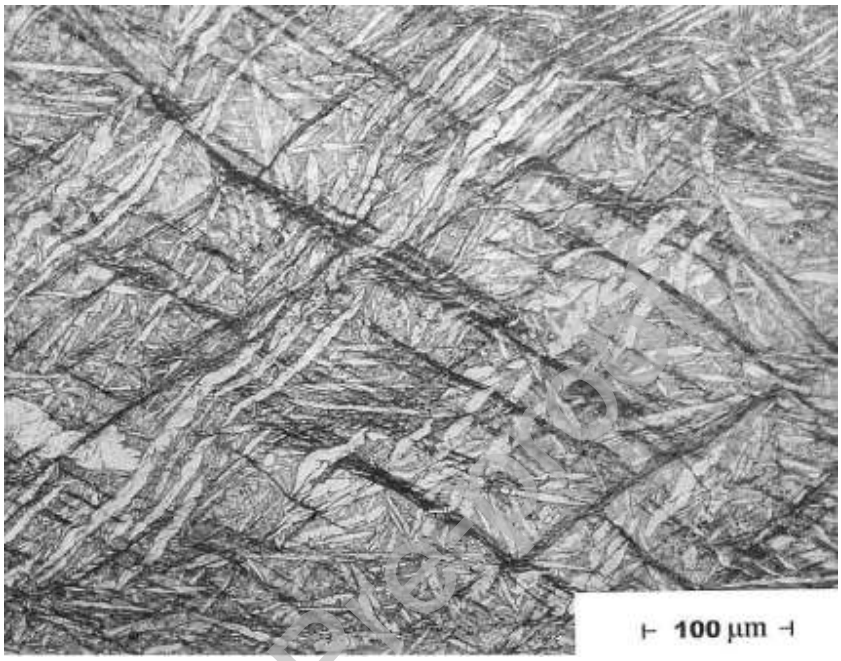

Figure, 19. U-0.75%Ti rolled to 40% reduction (true strain = 0.51) at 250°C. The dark diagonal features are bands of localized shear. The fact that martensite plates can be followed across these bands indicates that the amounts of shear strain in these bands are relatively modest. This is distinct from adiabatic shear instability, where enormous shear strains occur within very narrow bands, resulting in dramatic offsets across the bands.

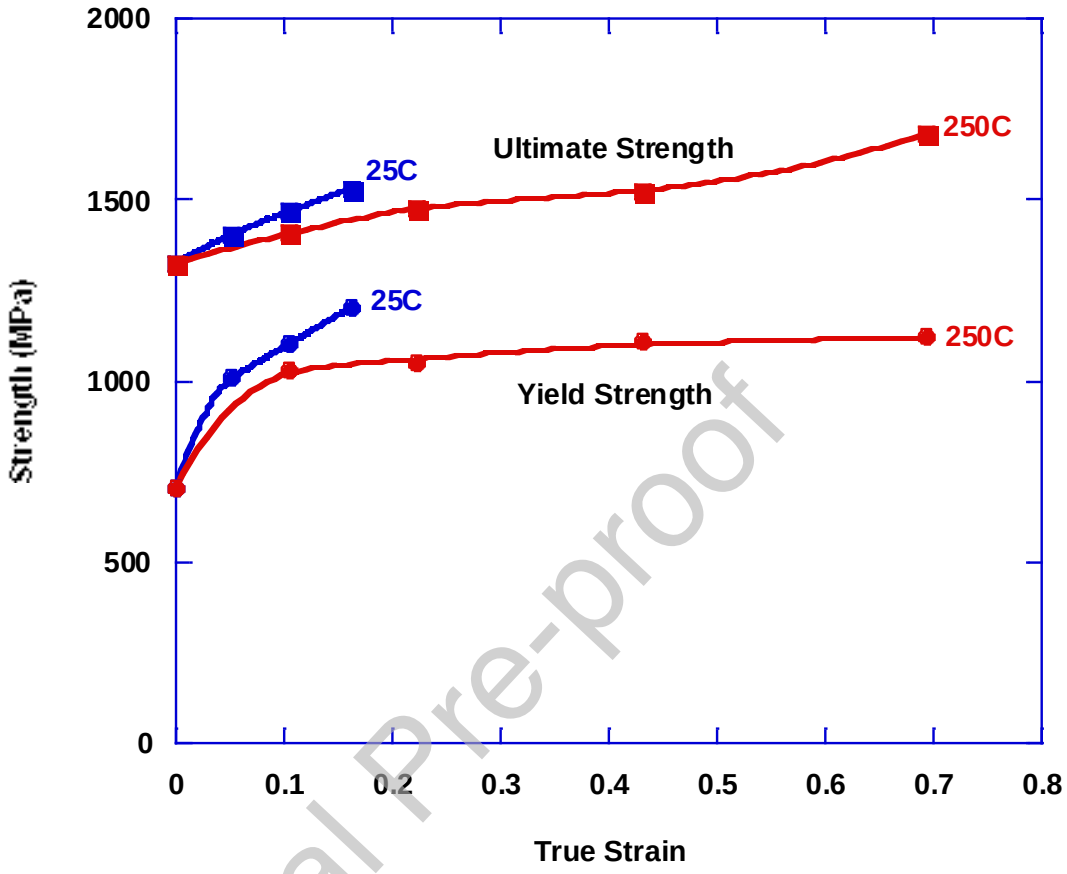

Figure 20. Effect of rolling on tensile yield and ultimate strengths of U-0.75%Ti. All data represents longitudinal samples taken parallel to the rolling direction. A limited number of transverse samples exhibited slightly lower yield and ultimate strengths (Table 3).

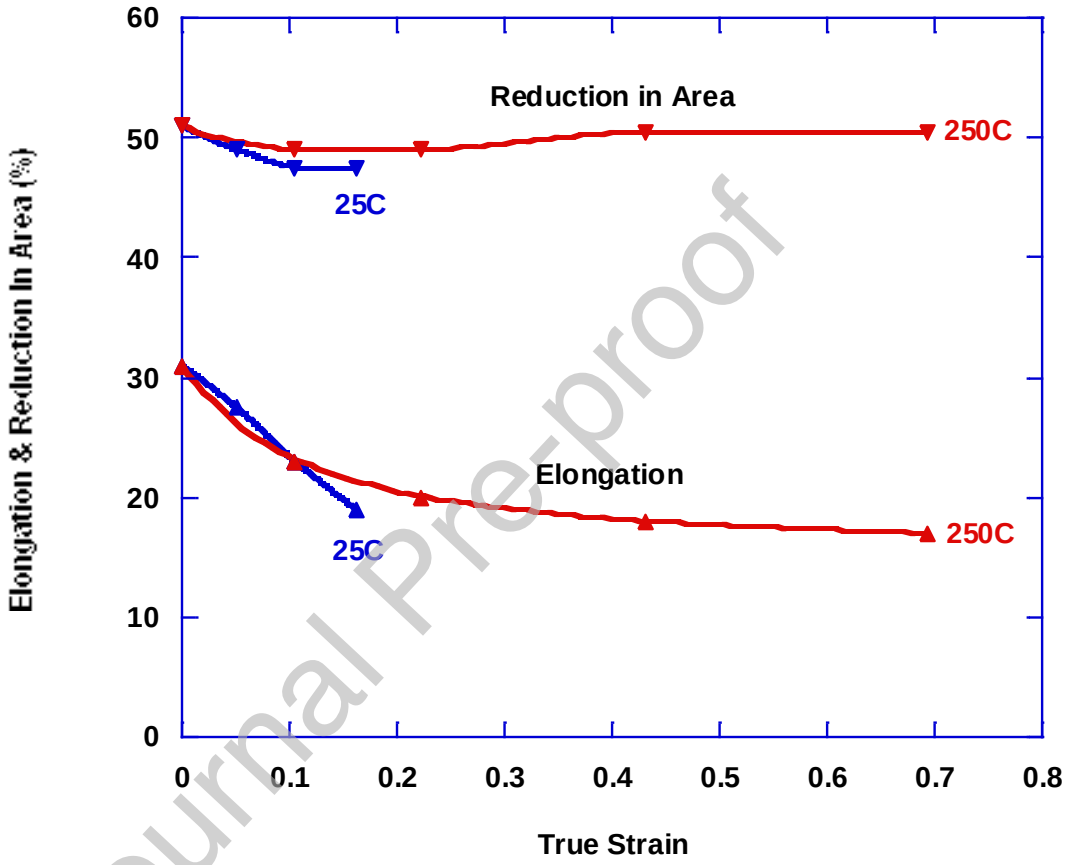

Figure 21. Effect of rolling on tensile elongation and reduction-in-area of U-0.75%Ti. All data represents samples taken parallel to the rolling direction. A limited number of transverse samples exhibited very similar elongations and reductions-in-area (Table 3).

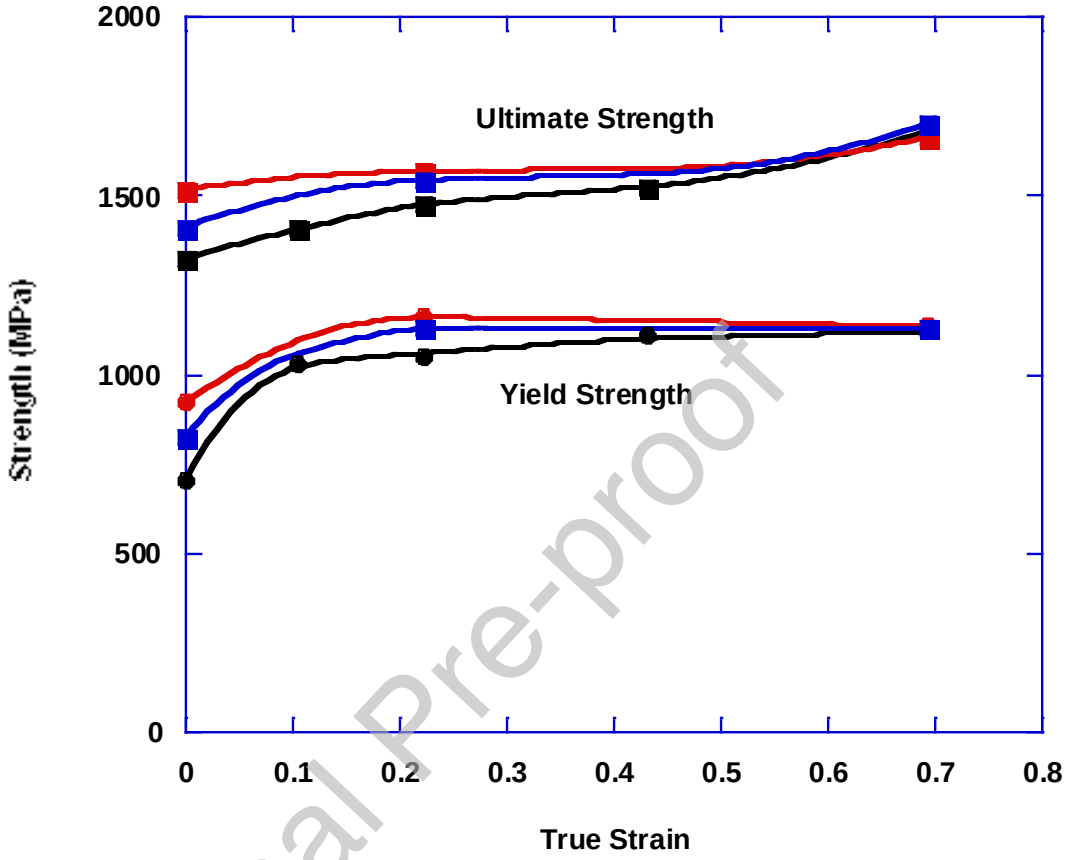

Figure 22. Effect of aging on tensile yield and ultimate strengths of U-0.75%Ti.

- Black: Rolled at 250°C, no subsequent aging.
- Blue: Rolled at 250°C, then aged at 380°C for 5 hours.
- Red: Rolled at 250°C, then aged at 400°C for 5 hours.
- Note that points at 0% deformation represent conventional age hardening.

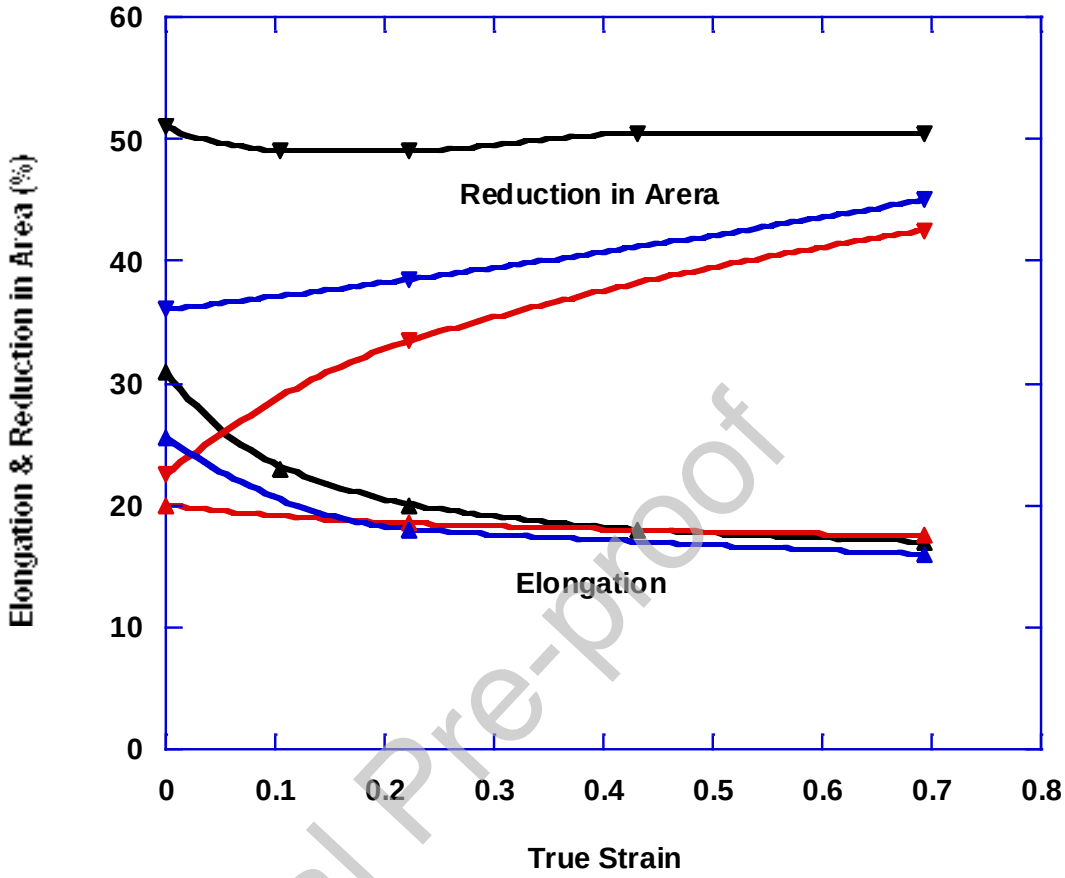

Figure 23. Effect of aging on elongation and reduction-in-area of U-0.75%Ti.

- Black: Rolled at 250°C, no subsequent aging.
- Blue: Rolled at 250°C, then aged at 380°C for 5 hours.
- Red: Rolled at 250°C, then aged at 400°C for 5 hours.
- Note that points at 0% deformation represent conventional age hardening.

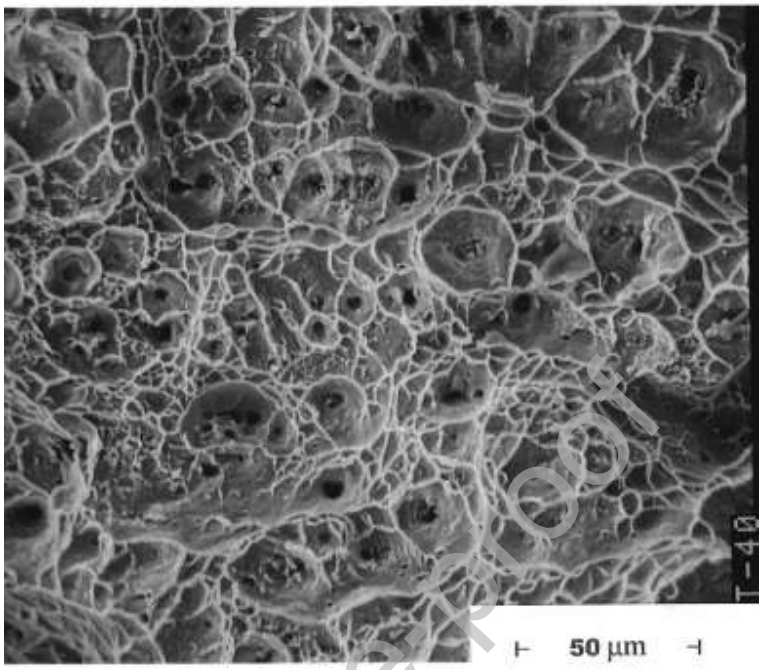

Figure 24. Fracture surface of undeformed (as-quenched) U-0.75%Ti tensile sample. Note coarse dimples indicative of failure by microvoid coalescence.

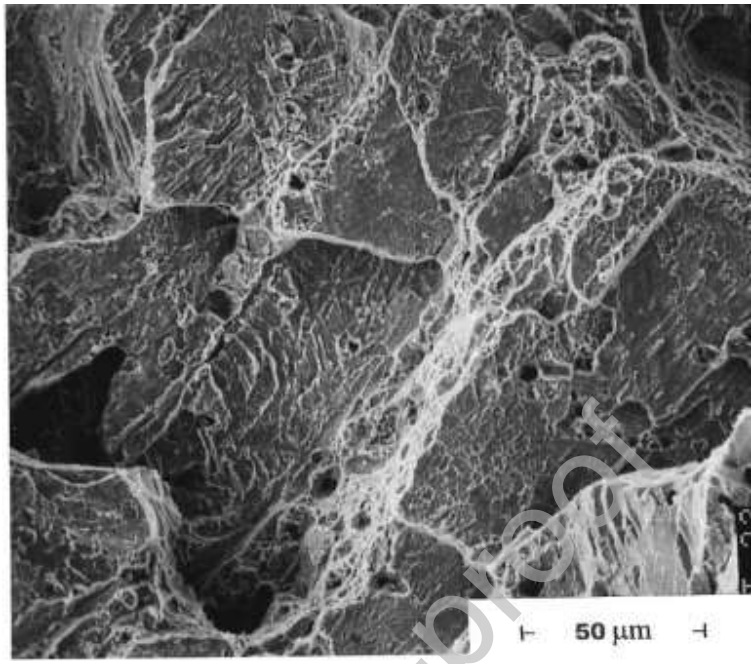

Figure 25. Fracture surface of undeformed U-0.75%Ti sample aged 400°C/6 hours. Note quasi-cleavage failure. Metallographic cross sectioning in this and other studies showed that the facets correspond to failure along the boundaries of martensite plates (Ref. 24).

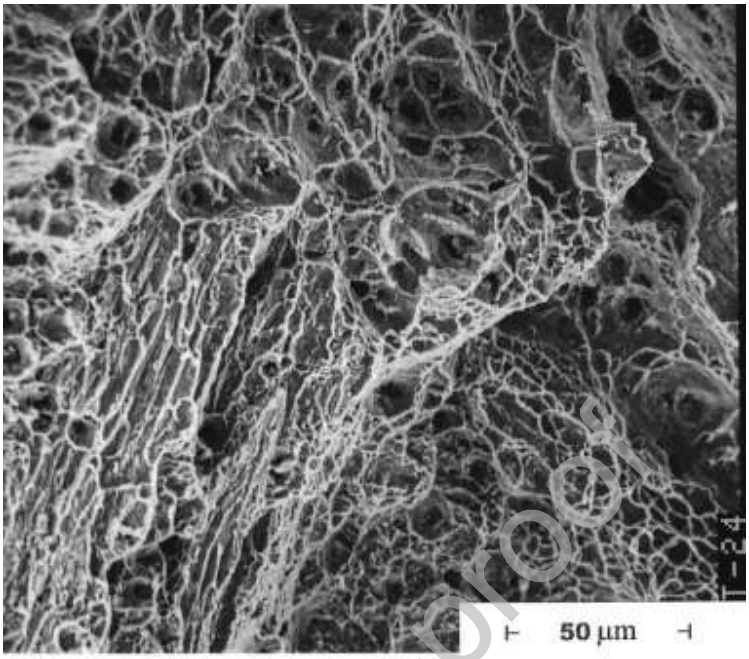

Figure 26. Fracture surface of U-0.75%Ti sample rolled to 10% reduction at 250°C then aged 400°C/6 hours. Note that failure occurred by a mixture of microvoid coalescence and quasi-cleavage.

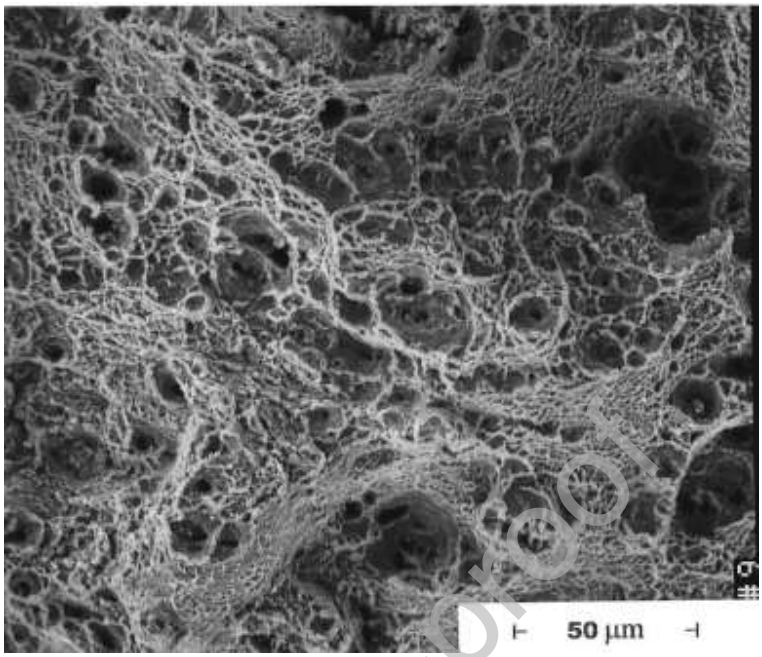

Figure 27. Fracture surface of U-0.75%Ti sample rolled to 50% reduction at 250°C then aged 400°C/6 hours. Note that failure occurred completely by microvoid coalescence, but with widely varying dimples sizes, many being very fine.

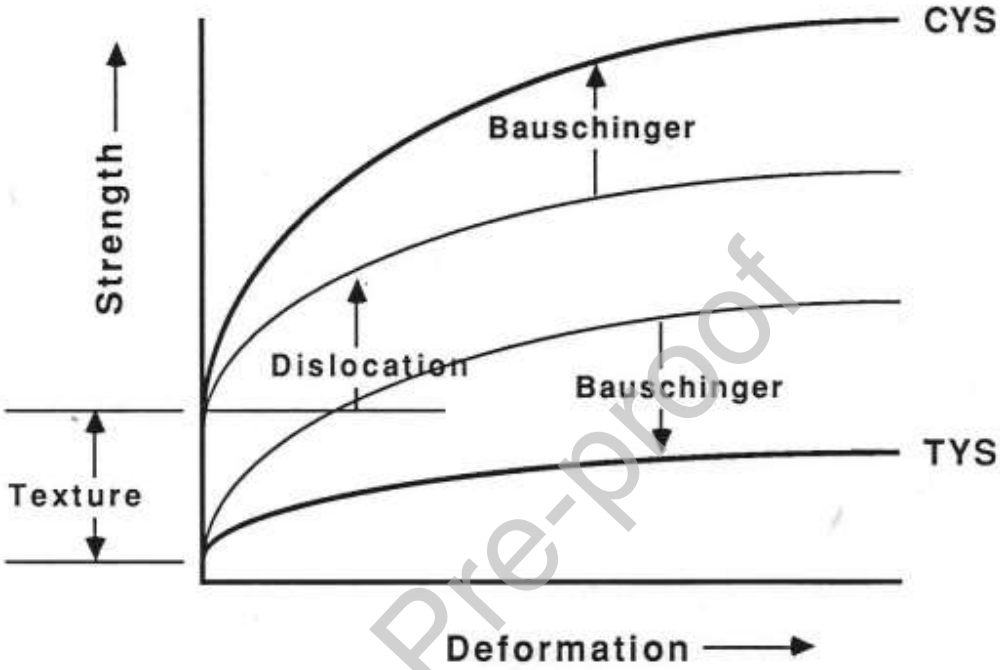

Figure 28. Components of deformation strengthening. This illustration describes what was observed for axial compressive deformation of U-0.75%Ti (compressive upsetting). The undeformed material exhibited higher axial yield strength in compression than in tension due to texture. Long-range dislocation strengthening occurred as a result of upsetting deformation, adding equally to axial compressive and tensile yield strength. The Bauschinger component added to axial compressive yield strength, but detracted from tensile yield strength. Conversely, rolling of U-2.3%Nb plate involved reduction in thickness but increases in length, similar to tensile strain parallel to the rolling direction. In this case the Bauschinger effect added to longitudinal tensile yield strength, but detracted from longitudinal compressive yield strength.

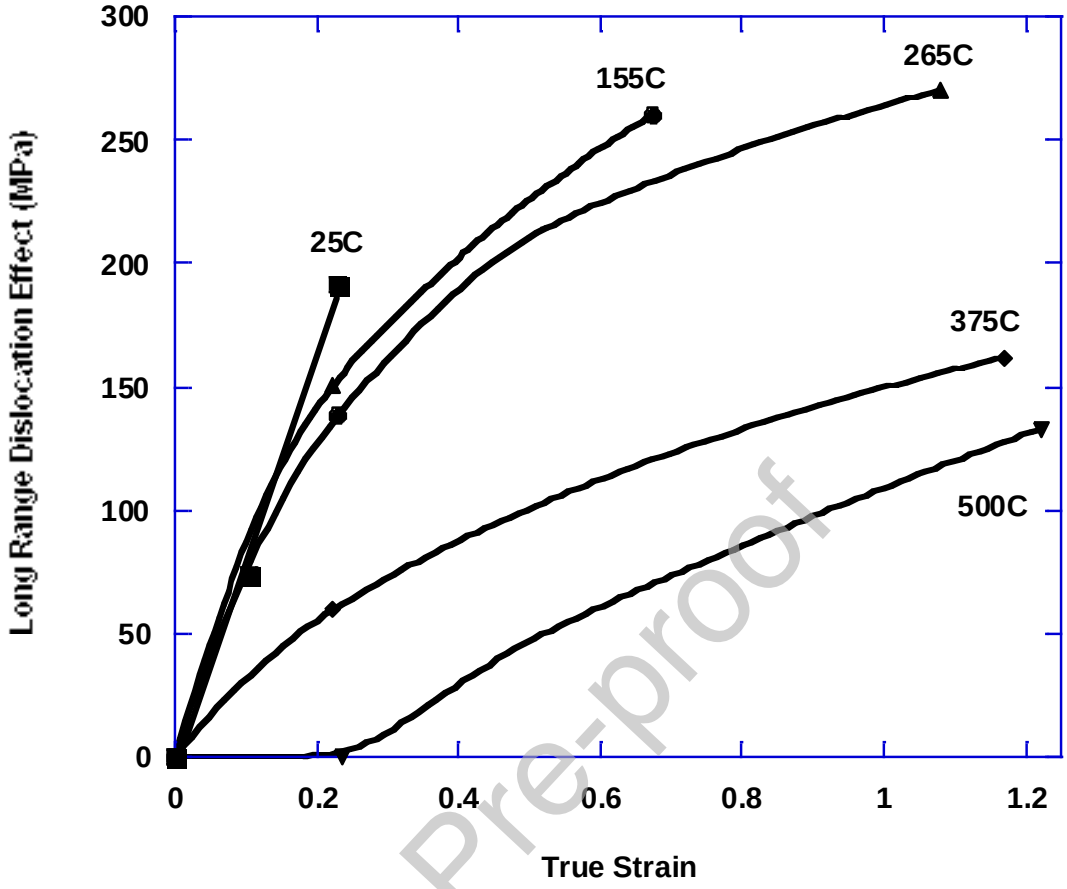

Figure 29. The effects of rolling temperature and strain on long-range dislocation strengthening in U-2.3%Nb

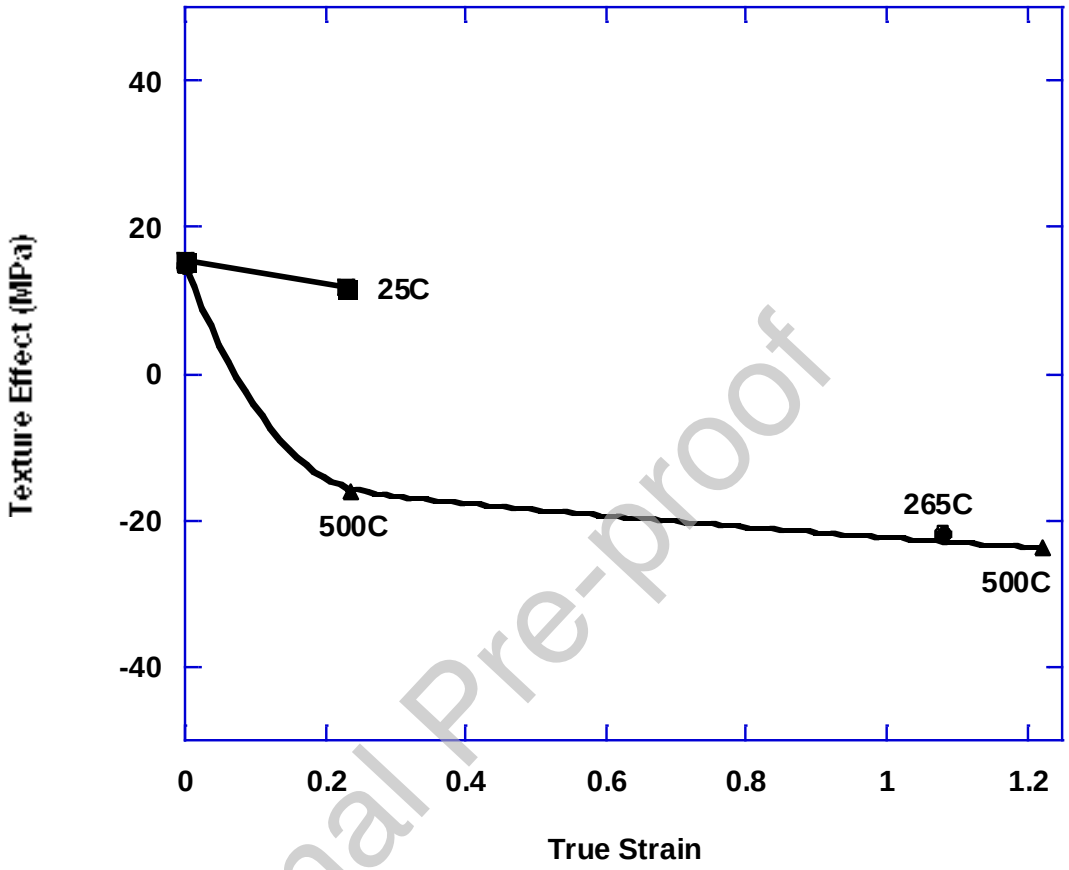

Figure 30. The effects of rolling temperature and strain on texture effect in rolled U-2.3%Nb.

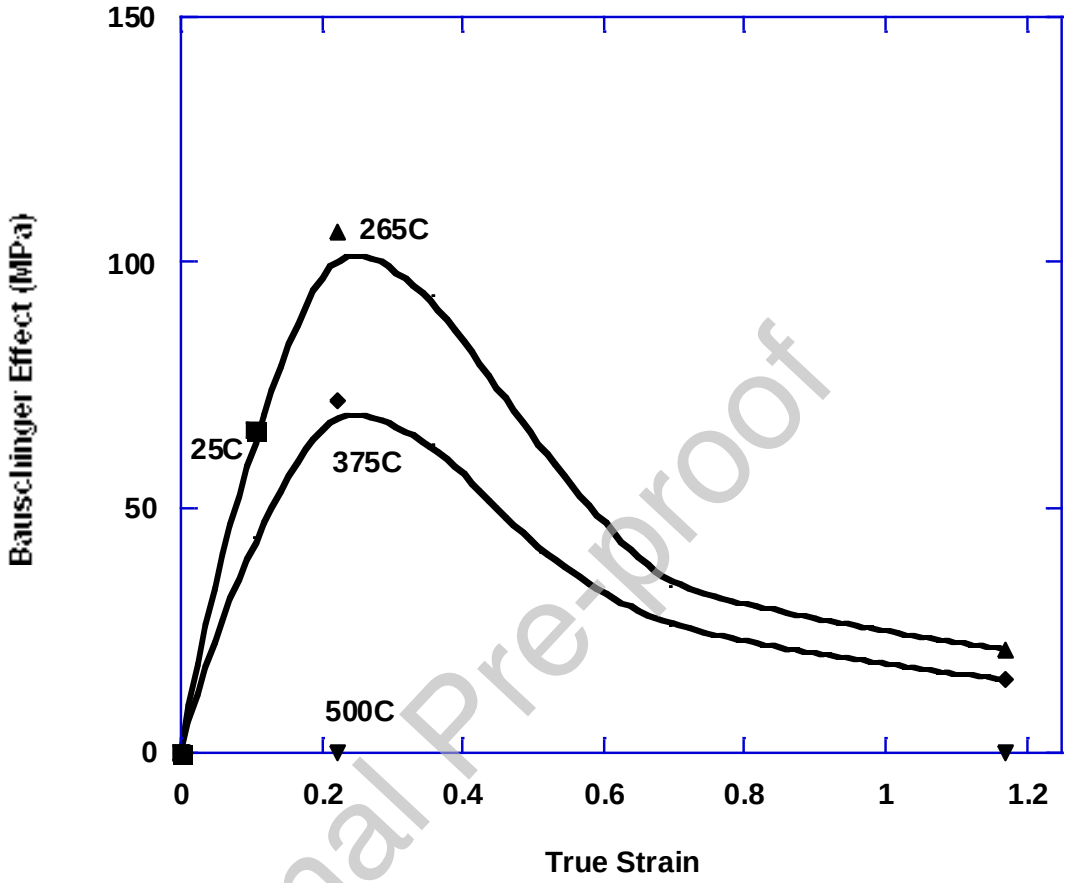

Figure 31. The effects of rolling temperature and strain on the Bauschinger effect in U-2.3%Nb.

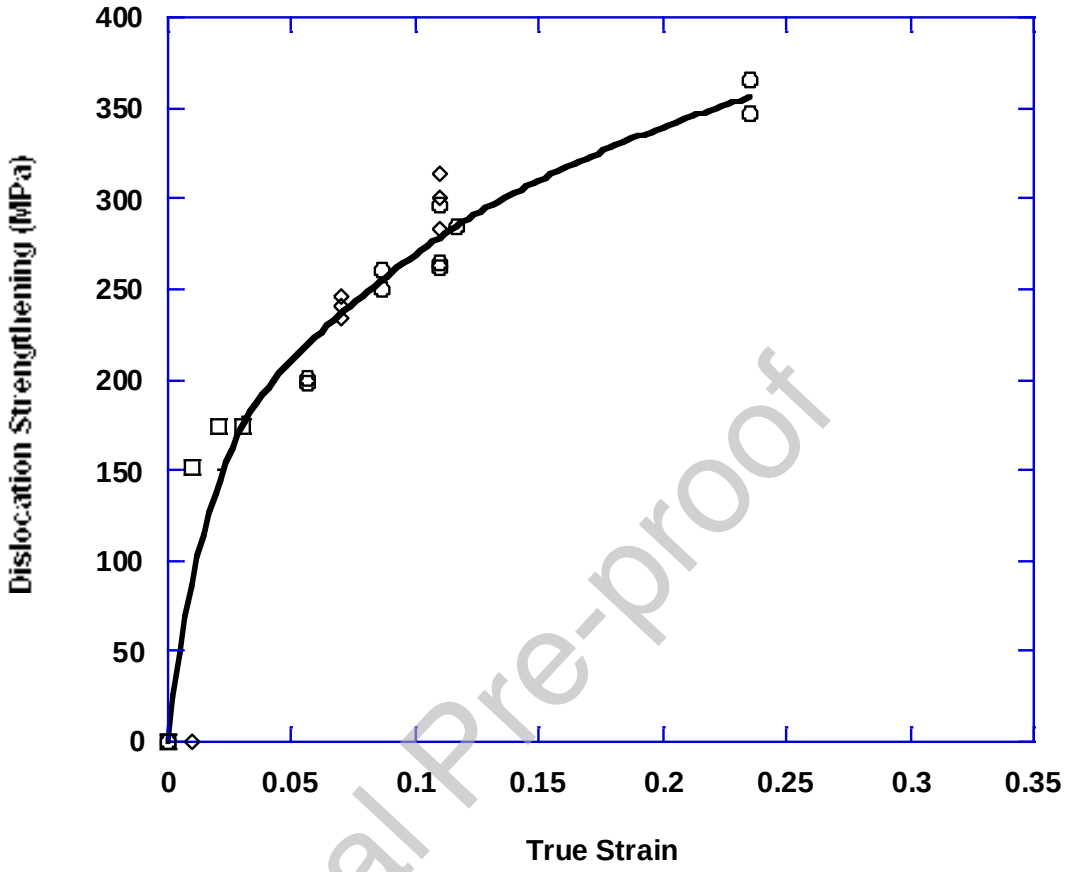

Figure 32. Long-range dislocation strengthening in U-0.75%Ti: comparison of aging before versus after deformation.
Squares: deformed at 25°C, then aged at 375°C (Ref. 8).
Circles: deformed at 25°C, then aged at 380°C (Ref. 34).
Diamonds: aged at 380°C, then deformed at 25°C (Ref. 34)

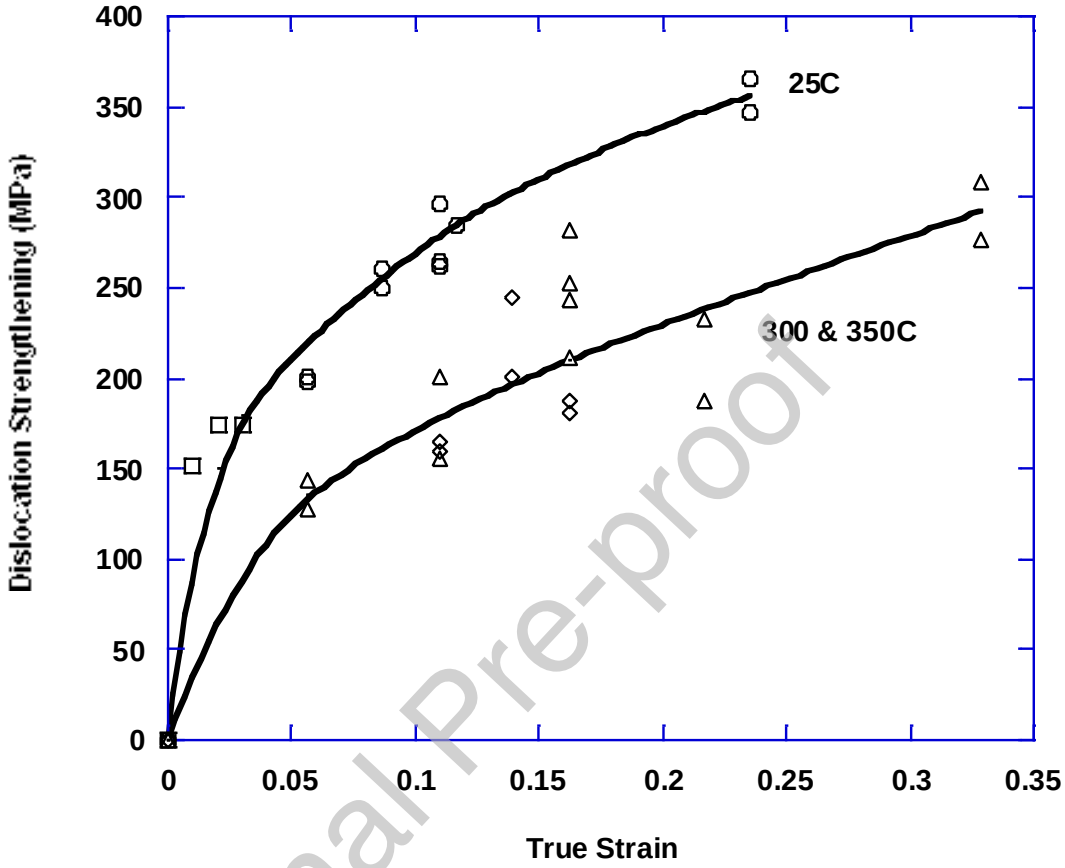

Figure 33. Effect of deformation temperature and strain on long-range dislocation strengthening in U-0.75%Ti. All aged at 375°C or 380°C after deformation.
Squares: Deformed at 25°C (Ref. 8)
Circles: Deformed at 25°C (Ref. 34)
Triangles: Deformed at 300°C (Ref. 34)
Diamonds: Deformed at 350°C (Ref. 34)

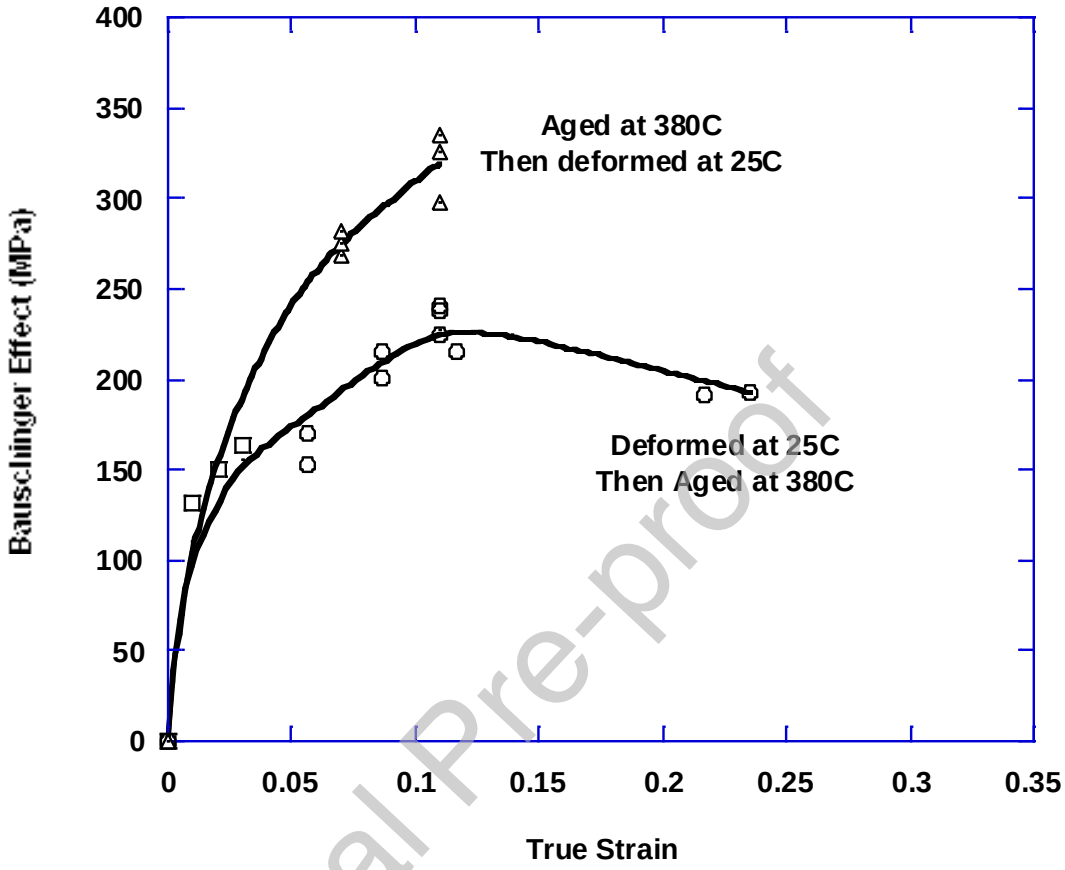

Figure 34. Bauschinger effect in U-0.75%Ti: comparison of aging before versus after deformation.
Triangles: Aged at 380°C, then deformed at 25°C (Ref. 34)
Squares: Deformed at 25°C, then aged at 375°C (Ref. 8).
Circles: Deformed at 25°C, then aged at 380°C (Ref. 34).

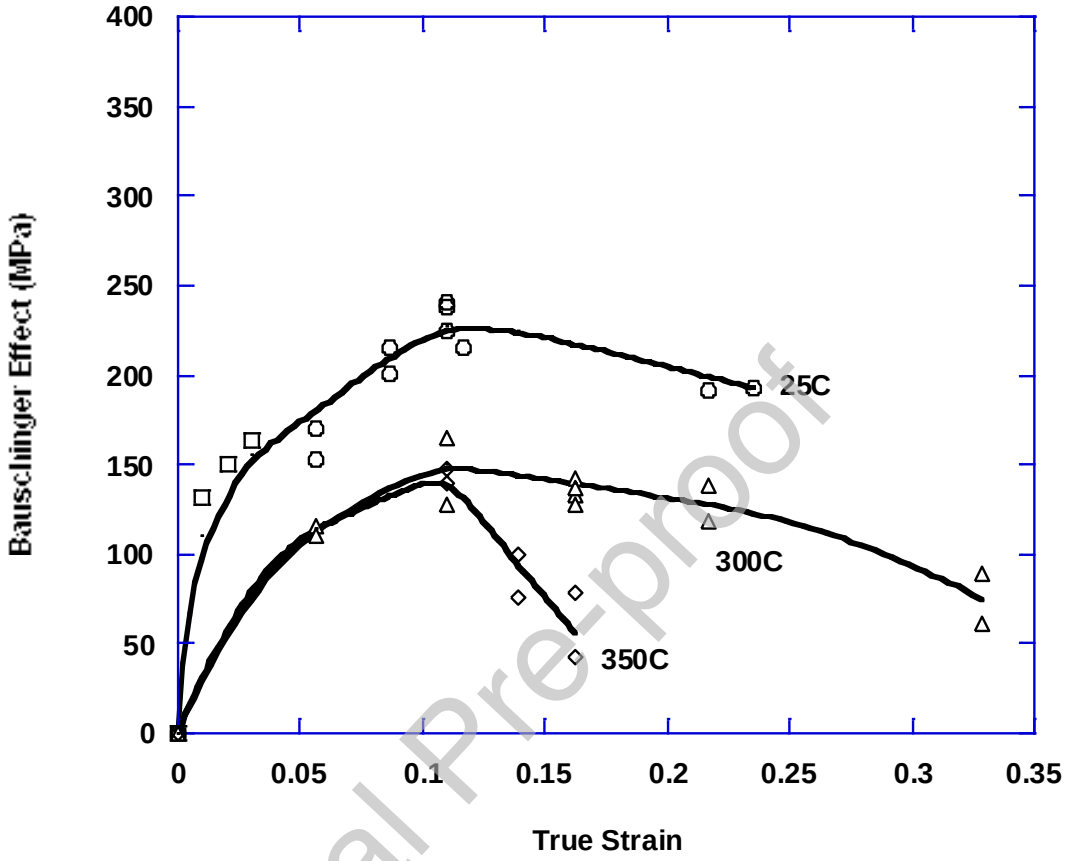

Figure 35. Effects of deformation temperature on long-range dislocation strengthening in U-0.75%Ti. All aged at 375°C or 380°C after deformation.
Squares: Deformed at 25°C (Ref. 8)
Circles: Deformed at 25°C (Ref. 34)
Triangles: Deformed at 300°C (Ref. 34)
Diamonds: Deformed at 350°C (Ref. 34)

Declaration-of-competing-interests

The authors declare that they have no known competing financial interests or personal relationships that could appear to influence the work reported in this paper.